Journal of Fluorescence (2023) 33:859–893
https://doi.org/10.1007/s10895-022-03135-6

REVIEW

Schiff Bases: A Versatile Fluorescence Probe in Sensing Cations

Neha Kumari[1] · Shalini Singh[1] · Minati Baral[1] · B. K. Kanungo[2]

Received: 21 October 2022 / Accepted: 24 December 2022 / Published online: 12 January 2023

Abstract
Metal cations such as Zn^{2+}, Al^{3+}, Hg^{2+}, Cd^{2+}, Sn^{2+}, Fe^{2+}, Fe^{3+} and Cu^{2+} play important roles in biology, medicine, and the environment. However, when these are not maintained in proper concentration, they can be lethal to life. Therefore, selective sensing of metal cations is of great importance in understanding various metabolic processes, disease diagnosis, checking the purity of environmental samples, and detecting toxic analytes. Schiff base probes have been largely used in designing fluorescent sensors for sensing metal ions because of their easy processing, availability, fast response time, and low detection limit. Herein, an in-depth report on metal ions recognition by some Schiff base fluorescent sensors, their sensing mechanism, their practical applicability in cell imaging, building logic gates, and analysis of real-life samples has been presented. The metal ions having biological, industrial, and environmental significance are targeted. The compiled information is expected to prove beneficial in designing and synthesis of the related Schiff base fluorescent sensors.

Keywords Schiff base · Fluorescent sensors · Cell-imaging · Metal ion recognition · Detection limit

Abbreviations

CHEF	Chelation enhanced fluorescence
FRET	Fluorescence resonance energy transfer
CHEQ	Chelation enhanced quenching
ICT	Intramolecular charge transfer
PET	Photoinduced electron transfer
ESIPT	Excited-state intramolecular proton transfer
LOD	Limit of detection
K_a	Association constant

Introduction

Recognition of metal ions has gained much attention among researchers in the past few decades due to their pertinence in pharmacology, biology, environment, catalysis, green chemistry, and analytical fields [1–6]. Metal cations such as Zn^{2+}, Al^{3+}, Hg^{2+}, Cd^{2+}, Sn^{2+}, Fe^{2+}, Fe^{3+}, and Cu^{2+} are required in essential biological processes involving oxygen transport, neurotransmission, energy production, synthesis of important molecules, regulation of gene expression and many more [7, 8]. At the same time, these metal ions are also lethal for the human body when not maintained in the proper concentrations. Both excess and deficiency of these metal ions lead to several hazardous diseases such as anemia, Parkinson's disease, Wilson's disease, Alzheimer's disease, Minamata, amyotrophic lateral sclerosis (ALS), Itai-Itai, reproductive disorders, kidney failure, prostate cancer, mental retardation, cardiac arrest [9–13]. The majority of these lethal ions, like Cr^{3+}, Hg^{2+}, Pb^{2+}, Sn^{2+}, Pd^{2+}, Cd^{2+}, and Ni^{2+}, are essential in the industries such as the food, textile, paper industries, pharmaceuticals, metal refineries, electronic fields and construction of batteries, from which they are released into the water bodies and soil thereby harming the plants and aquatic life [14–19]. Hence, there is a tremendous demand to emphasize the development of fast-detecting devices for monitoring the concentration of these toxic ions. Currently, there are several techniques, such as atomic absorption-spectroscopy (AAS), inductively coupled mass-spectrometry (ICPMS), voltammetry, and UV–visible absorption spectroscopy used for detecting the metal ions, but these techniques are expensive, time-consuming, less sensitive and have a complicated procedure [20–22]. So, to overcome these limitations, chemosensors of different kinds have been developed and explored for their metal ions recognition properties. A chemosensor, used in qualitative or quantitative detection of a specific chemical substance, is comprised of three elements: a receptor responsible for the selective analyte binding, a photoactive unit whose properties depend upon this selective

✉ Minati Baral
minatibnitkkr@gmail.com

[1] National Institute of Technology, Kurukshetra Haryana-136119, India

[2] Sant Longowal Institute of Engineering and Technology, Longowal, Sangrur Punjab-148106, India

analyte binding, and a spacer that can change the geometry of the system and tune the electronic interaction between the two former moieties. Depending on the nature of the signal emitted by the signaling subunit, chemosensors can be classified into three categories: (i) colorimetric sensors, which are related to changes in electronic properties via different charge transfer processes accompanying color change (ii) electrochemical sensors, includes the change in redox potential which triggers signal production (iii) Fluorogenic sensors, whose signals are affected by various processes including chelation enhanced fluorescence (CHEF), fluorescence resonance energy transfer (FRET), intramolecular charge transfer (ICT), excited-state intramolecular proton transfer (ESIPT), C = N isomerization and photoinduced electron transfer (PET), excimer-exciplex formation [23–25]. The field of molecular monitoring by fluorescent probes has slowly become a hotspot in the environment, biology, and material science due to the ease of production, non-destructiveness, quick response, low cost, high sensitivity and sensitivity and selectivity towards toxic ions. Great efforts are being made to advance fluorescent detectors for metal cations due to their potential applications in real-time sample analysis, biological fluorescence imaging, molecular catalysis, and logic gate construction [26–33]. To this end, Schiff base derivatives play a crucial role in ion recognition, mainly in developing fluorescent chemosensors. These compounds gained much attention from researchers because of their easy methods of preparation, availability, and ability to complex with almost every metal ion [34, 35].

Schiff bases, also known as imines or azomethines, are nitrogen analogs of aldehyde or ketone with the replacement of the carbonyl group by the imine group [36, 37]. They are represented by the standard formula $R_1R_2C=NR_3$, while in some cases, this carbon atom is bonded with the hydrogen atom representing the formula $R_1CH=NR_2$ where R_1, R_2, or R_3 are the organic side chains (alkyl or aryl groups) [38–40]. These compounds play a substantial role in the purification of metals, electroplating, organic synthesis, metallurgy, photography, and the analytical field. The Schiff bases' coordination chemistry fascinated researchers because of its diversified applications in industries such as pigments, dyes, intermediates, polymer stabilizers, catalysts, and corrosion inhibitors. Further, these Schiff bases play wide roles in biological systems as they possess anti-inflammatory, antifungal, antibacterial, analgesic, antioxidant, cardiovascular, and antitumor properties and act as local painkillers [41–50].

Schiff Base Fluorescent Chemosensors

Fluorescent chemical sensors are the molecules that show changes in the fluorescence characteristic properties in response to an analyte. Depending on the nature, these sensors can detect different types of analytes, such as cations, anions, neutral molecules, or gases. Schiff base fluorescent sensors can detect different types of cations over other compounds due to the number of binding sites; unique cavity sizes available where the metal cation can efficiently bind and forms a stable complex. Other structural factors include the size and charge of the ion, electron configuration, and hard and soft acid–base characteristics of both the cation and donor sites in the Schiff base. Some recent research on Schiff base fluorescent sensors containing binding sites such as furan [51], imidazole [52], anthracene [53], pyridine [54], benzopyran, phenanthroline, neocuprine [55], coumarin [56], metal nanoparticles in sensors [57, 58] is well documented in the literature. Synthesis, properties, and fluorescence mechanisms of Schiff base compounds are also discussed in detail [59, 60]. In the earlier reported reviews [61–66], the reviewers covered all the biomedical and industrial applications of Schiff bases. Studies were also documented, which covered anion sensing by colorimetric, pH-sensitive, and fluorescent Schiff base sensors for cell imaging and applications of optical sensors.

This current review is consciously focused on the development of Schiff base fluorescent chemosensors for biologically, industrially, and environmentally essential cations such as Zn^{2+}, Al^{3+}, Hg^{2+}, Cd^{2+}, Pb^{2+}, Fe^{2+}, $Fe^{3+}$and Cu^{2+}. After conferring the literature, this review summarizes the literature from 2016 and ahead. The present review provides detailed mechanisms involved in sensing metal cations along with their structures, binding stoichiometries, association constant, the limit of detection, and synthesis schemes for some of the sensors. The practical applicability of different sensors, such as cell imaging, logic gate construction, paper strip tests, and analysis of wastewater samples, is also given with the respective sensors. In the end, these sensors' applications, advantages, and disadvantages are discussed.

Fluorescence Sensors for Al (III)

Aluminum, a majorly used element in our day-to-day life, is the third most abundant metal in the earth's crust and has many applications in biology, the environment, and industries. This metal is used mainly in making products such as aluminum foils, window frames, utensils, airplane parts, etc., due to its lightweight, malleability, and soft nature. Aluminum accumulation has increased dramatically in the environment yearly due to human activity and acid rain. Although Aluminum is a non-essential element, it can potentially produce toxicity and accumulate in the human body. When aluminum reaches the blood circulation system, it gets into tissues and cannot get excreted. The standard intake (WHO report) of aluminum in the human body is 3–10 mg per day, and its permissible limit

in drinking water is 7.4 l M. Excessive intake of aluminum leads to joint pain, myopathy, dementia, Alzheimer's, and Parkinson's diseases [67–69]. So, the detection of Aluminium by potentially selective chemosensors is necessary. Some most promising Schiff base fluorescent sensors for selective detection of aluminum have been analyzed and reported below.

Fan et al. developed a chromone-based Schiff base (1), which shows turn-on fluorescence in the presence of Al^{3+} metal ions [70]. The molecule displayed a 500-fold enhancement in fluorescence intensity along with a noticeable color change from colorless to yellow-green in ethanol upon binding with Al^{3+}, having the excitation and emission wavelengths as 423 nm and 507 nm, respectively. It also showed high sensitivity in ethanol with a detection limit of 5×10^{-8} M, which is sufficiently low to detect the sub-micromolar concentration of Al^{3+}. This enhancement in emission intensity was due to the blocking of the PET mechanism, i.e., the lone pair of nitrogen that were freely available for donation are no more available after complexation with metal Al^{3+} ion, thereby restricting the electron transfer process. Also, ML_2-type complex formation between the aluminum ion and the ligand leads to rigidity in the structure, resulting in chelation-enhanced fluorescence (CHEF) [Fig. 1].

Boron-dipyromethane (BODIPY) based Schiff bases (2) and (3) comprising quinoline and pyrazine moieties were reported for the selective detection of aluminum in the acetonitrile–water medium [71]. (2) and (3) showed a color change from pink to green on adding an excess amount of Al^{3+} which is possibly due to the hydrolysis of the imine bond. Both probes encapsulate aluminum ions through hydrogen bonding. These sensors showed weak fluorescence because of intramolecular charge transfer (ICT) between the BODIPY and hydrazine functionality. After the addition of Al^{3+}, an increase in emission intensity of the band present at 552 nm from 220–290 a.u for (2) and 220–610 a.u for (3) was observed. In another work, a polymer-based fluorescent chemosensor (4) was synthesized by post-modification of poly (ethylene glycol) using salicylaldehyde-based Schiff base derivate and elaborated for its magnificent selectivity and sensitivity towards Al^{3+} in pure aqueous media [72]. Its solution in free form exhibited negligible fluorescence, but as Al^{3+} was added to the solution, an apparent increase in the fluorescence (up to 490 a.u) emission was induced with the peak centered at 459 nm, and the solution also displayed a drastic color change from colorless to bright cyan. Several other metal cations had little interference with the fluorescence intensity of the probe. Test strips coated with the molecule (4) were also made for checking Al^{3+} concentration in real water samples, and they could also be used to construct inhibit-type logic gates. Similarly, by modification of poly-(ethylene glycol) with thiophene Schiff base derivative, a fluorescent turn-on chemosensor (5) was synthesized [73]. (5) reports selective and sensitive determination of Al^{+3} over a wide pH range in the presence of other metal ions in an aqueous medium. This water-soluble chemosensor had a detection limit of 1.32×10^{-8} M, which was way lower than the maximum concentration of 7.41 µM of Al^{3+} in drinking water recommended by WHO. Two isomeric antipyrine derivatives (6) and (7), on binding with Al^{3+}, regardless of the orientation of the naphthol ring, experienced nearly 25-fold and fourfold enhancement, respectively [74]. The visible color change was shown by chemosensors through PET on binding with Al^{3+} making them suitable colorimetric sensors. These isomers were applied in constructing 'AND' type logic gates by providing EDTA and Al^{3+} as inputs. Structures of the sensors (2)-(7) are shown in Fig. 2. Also, Table 1 lists various characteristic properties of chemosensors (2)-(7).

Schiff base (E)-4-methyl-2-((2-(9-(naphthalen-1-yl)-8-(thiophen-2-yl)-9H-purin-6-yl)hydrazono) -methyl) phenol,(10) (a yellow colored solid having 85% yield) was derived from 6-hydrazinyl-9-(naphthalen-1-yl)-8-(thiophen-2-yl)-9H-purine (8) (200 mg, 0.558 mmol) and 2-hydroxy-4-methylbenzaldehyde(9) (114 mg,

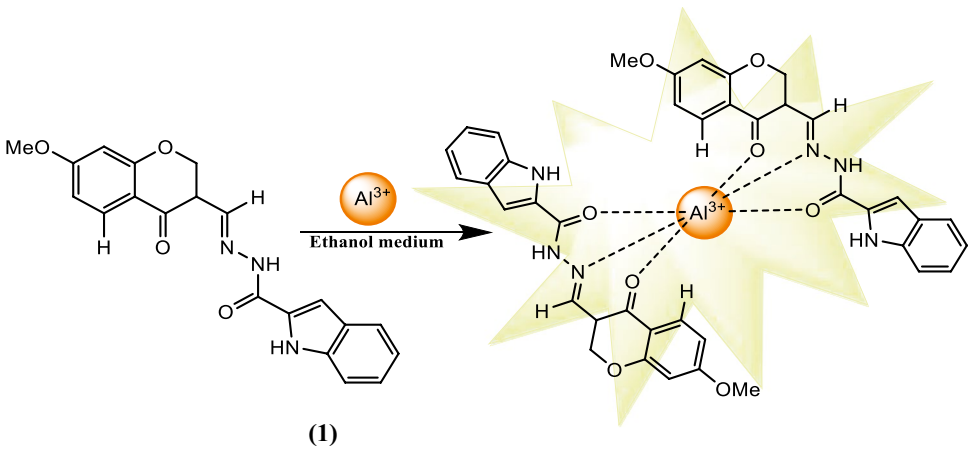

(1)

Fig. 1 Plausible sensing mechanism of (1) for Al^{3+}

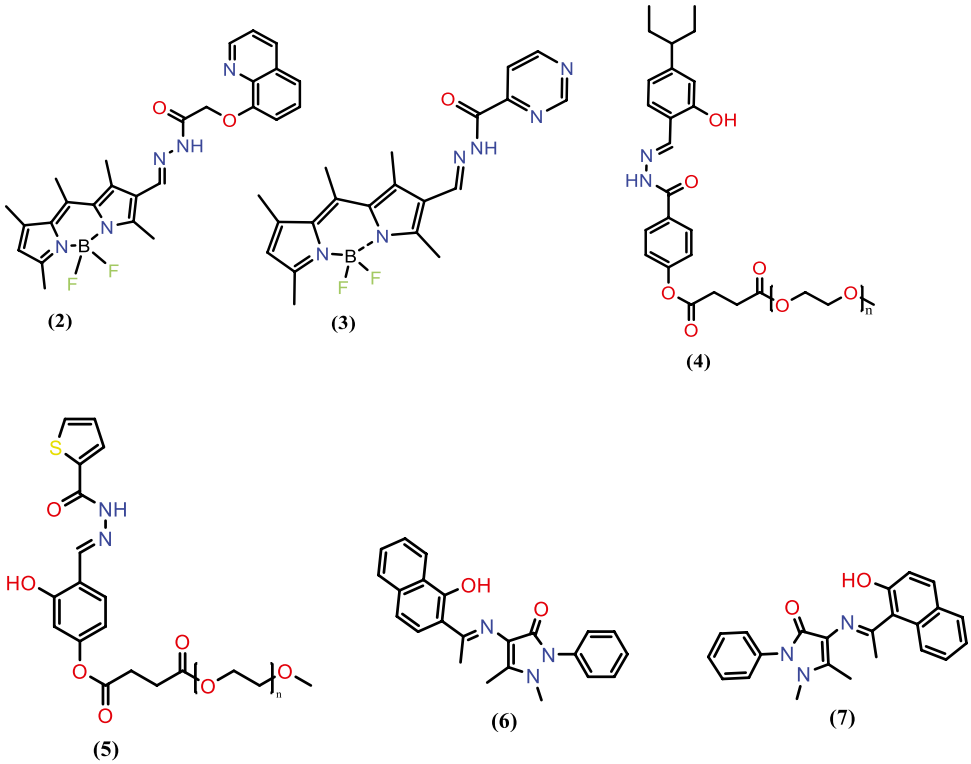

Fig. 2 Structures representing Chemosensors (2), (3), (4), (5), (6), and (7)

0.837 mmol) after refluxing for two hours in an ethanolic medium as represented in Scheme 1 [75]. (10) was efficiently employed for detecting trace Al^{3+}in living HeLa cells via cell imaging experiments by developing test strips. The fluorescence intensity enhanced up to 3×10^5 a.u upon adding Al^{3+} and a visual color change from colorless to pale yellow.

Another fluorescence turn-on compound (11), which employed a terpyridine-based Schiff base, showed very weak emission at 528 nm when excited at 265 nm [76]. Upon the addition of Al^{3+}, a 51-fold enhancement in the fluorescence, along with a hypsochromic shift (516 nm) was observed. This can be explained on account of strong intramolecular charge transfer and hindrance of PET and C = N isomerization process [Fig. 3]. The NMR and Job's plot results revealed that Al^{3+} binds with the ligand in a 2:1 ratio forming the M_2L-type complex. The LOD and association constant were found to be 3.32×10^{-7} mol L^{-1} and 6.8×10^5 M^{-1} respectively.

A steroid-based Schiff base (12) was developed through microwave-assisted synthesis that showed high fluorescence selectivity towards Al^{3+} in an ethanol–water (1:2) solvent system [Fig. 4a] and, thus, applied in sensing Al^{3+} in actual water samples [77]. The detection limit was low (34 nM) in the pH range of 6.05—9.32. Banerjee and co-workers reported an N_2O_2 donor Schiff base (13) with an azo arm that selectively detects Al^{3+} in a semi-aqueous medium [78]. The fluorescence studies of (13) revealed weak fluorescence at 510 nm on excitation at 388 nm. Upon addition of Al^{3+} ions, 61-fold fluorescence enhancement along with a blue shift from 510 to 478 nm was seen, despite the presence of other metal ions. It was successfully employed in the development of an inhibition-type molecular logic gate and sensing Al^{3+} in fewer organic solvents. Schiff

Table 1 Some characteristic properties and the binding mechanism for (2)-(7)

Cation sensor	$\lambda_{ex}/\lambda_{em}$ (nm)	M:L ratio	Binding constant(M^{-1})	Detection limit (M)	Mechanism	Reference
(2)	360/552	1:1	5.5×10^4	86.6×10^{-8}	ICT, CHEF (turn-on)	[71]
(3)	360/552	1:1	6.6×10^4	13.7×10^{-8}	ICT, CHEF (turn-on)	[71]
(4)	394/459	1:1	1.01×10^5	2.93×10^{-9}	CHEF (turn-on)	[72]
(5)	374/444	1:1	8.74×10^4	1.32×10^{-8}	PET, C = N, CHEF (turn-on)	[73]
(6)	400/576	1:1	6.03×10^3	1×10^{-5}	PET, CHEF (turn-on)	[74]
(7)	400/576	1:1	5.56×10^3	5×10^{-10}	PET, CHEF (turn-on)	[74]

Scheme 1 Scheme for the synthesis of (10)

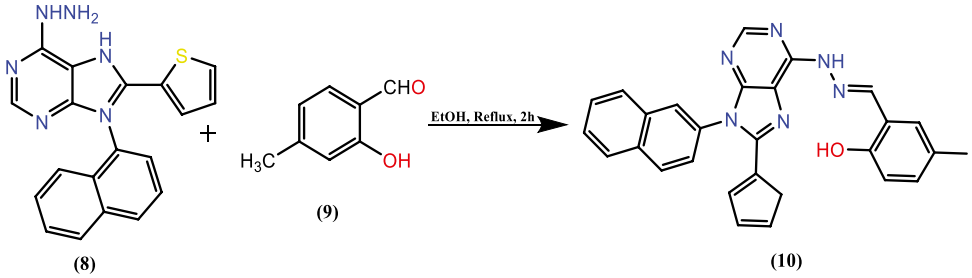

base (E)-N′-(4(diethylamino)-2-hydroxybenzylidene)-2-hydroxybenz-ohydrazidebenzylidene-based (14) having potential biomedical applications, shows a 45-fold increase in fluorescence intensity on complexing with Al^{3+} ion due to development of rigid system causing chelation enhanced fluorescence [Fig. 4b] [79]. The detection limit was very low for sensing Al^{3+} (3.60×10^{-6} M). The Benesi–Hildebrand expression gave the stability constant value as 1.21×10^{5} M^{-1} with the stoichiometric ratio 1:1 for the metal: ligand complex. The fluorescence studies of another Schiff base (15) were done in DMF: water (9:1) as a solvent system, which suggested that (15) in its free form emitted negligible fluorescence but in the presence of Al^{3+}, a 34-fold enhancement in fluorescence was noted, which is due to strong ICT and CHEF effects taking place in the complex [80]. The stoichiometry of the ligand-Al^{3+} complex was 1:1, and the limit of detection calculated was 6.7 µM. The sensor could be recycled by using appropriate complexing agents such as EDTA due to its reversibility. Structures of the above-mentioned Schiff bases are shown in Fig. 5.

To increase the water solubility, Hwang and the group have used aminobenzoic acid for the synthesis of Schiff base (16) through a simple condensation process [81]. This showed better and more efficient recognition of Al^{3+} ions [Fig. 6b] in aqueous media amongst other metal cations, i.e., Mn^{2+}, Fe^{3+}, Co^{2+}, Ni^{2+}, Cu^{2+}, Zn^{2+}, Cd^{2+}, Hg^{2+}, Na^{+}, K^{+}, Mg^{2+}, Ca^{2+}, Pb^{2+} and Cr^{3+} which caused minor changes in fluorescence. Based on the results from fluorimetric titrations and Job's plot, the structure of (16)-Al^{3+} complex was proposed, as shown in Fig. 6a. The binding constant calculated was very high (3.1×10^{8} M^{-1}), and the LOD reported was very low (290 nM).

Schiff base (17), a brown-colored solid, was synthesized by refluxing salicylidene-4-aminoantipy–rine and 4-aminophenol for 6 h in an ethanolic medium with 52% yield and was characterized by IR, NMR, and mass data [82]. This compound (17) displayed no fluorescence, but on binding with aluminum ions, the fluorescence intensity increased up to 690 a.u. Due to the formation of the complex, the ESIPT mechanism gets hindered as the hydrogen

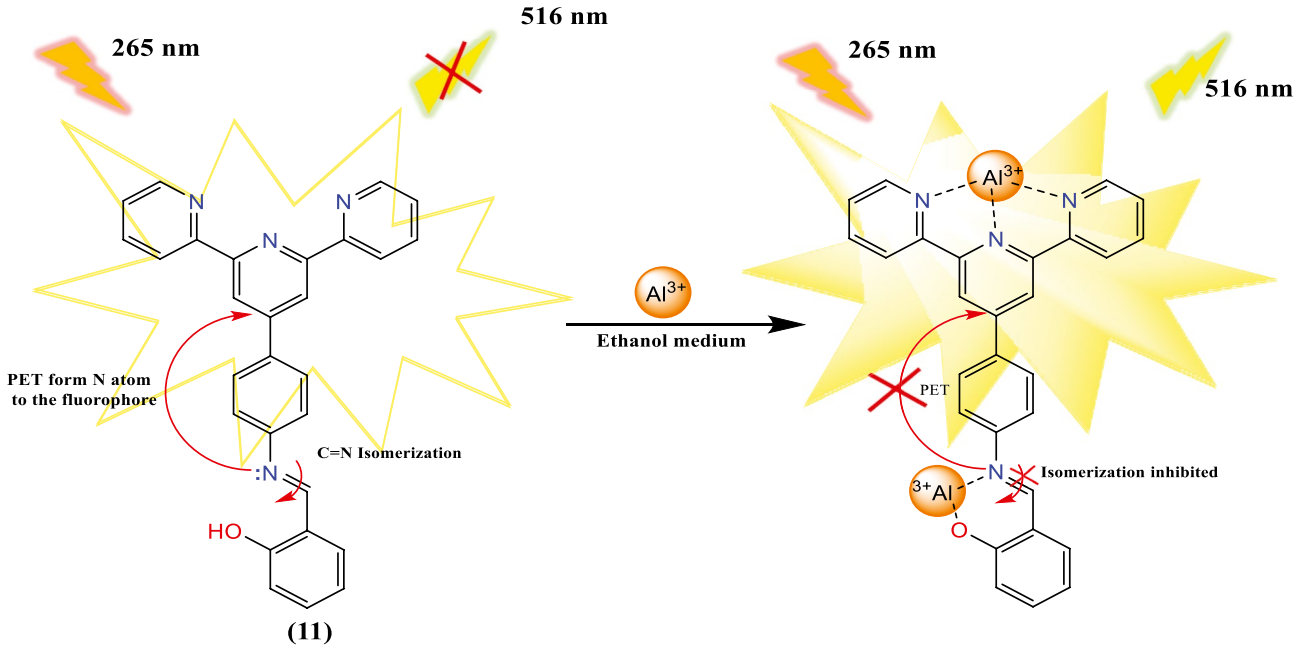

Fig. 3 Binding mechanism of the sensor (11) with Al^{3+} ion

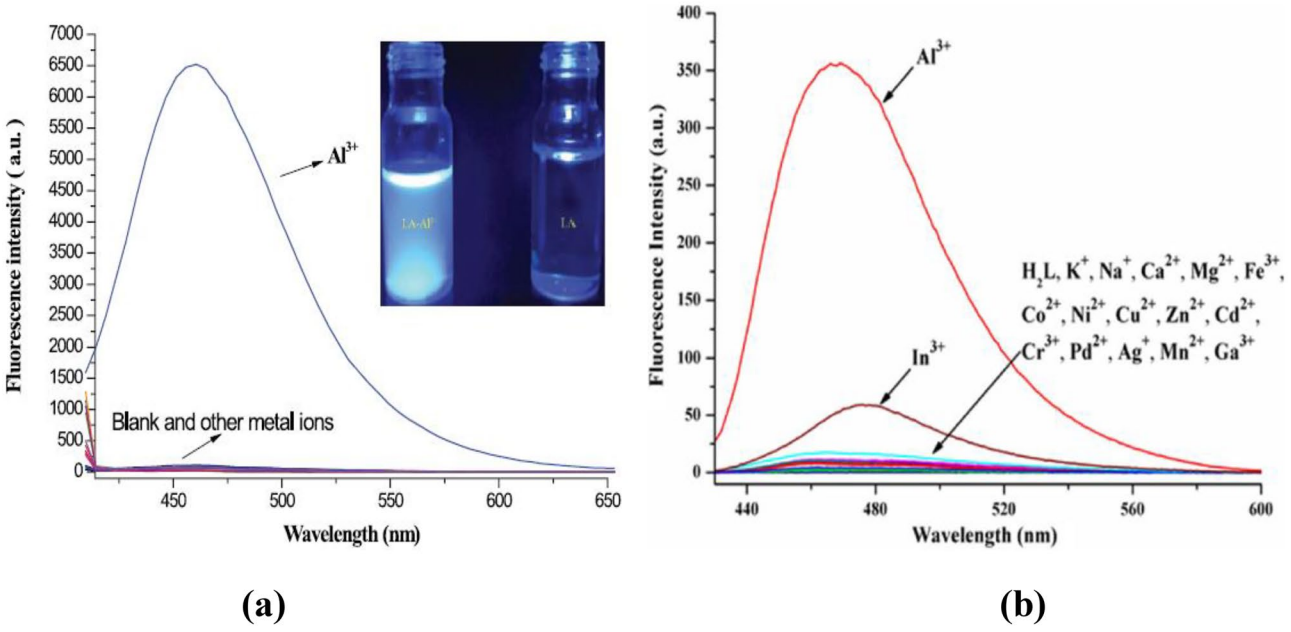

Fig. 4 Fluorescence spectra of **a** sensor (12); **b** sensor (14) with different metal cations

involved in hydrogen bonding was removed during complex formation, followed by the electron transfer process. A phenyl thiadiazole-based Schiff base receptor (18) was developed for colorimetric as well as fluorometric detection of Al^{3+} in a methanol-tris–HCl buffer medium [83]. The sensor displayed fluorescence to 5000 a.u on exciting at 310 nm, which increased up to 15,000 a.u with Al^{3+} ions accompanying a color change from colorless to bright yellow.(18) can be potentially used in the construction of binary logic gates, smartphone-based chemical analysis, and recovery of contaminated water due to quick fluorometric response time. Another turn-on fluorescent sensor (19) was found to be an effective fluorometric probe for sensing Al^{3+} ions [84]. Molecule (19), along with Al^{3+}ions, also acts as a colorimetric sensor for Fe^{2+} and Fe^{3+} (yellow to brown for both). This probe showed an 18-fold enhancement in the presence of Al^{3+}ions. A cis-dioxo molybdenum (VI) complex derived from multidentate hydrazone ligand (20) was investigated for its fluorescence properties in an aqueous-DMF medium which revealed its

Fig. 5 Structures of fluorescent chemosensors (12)-(15) used for selective detection of Al^{3+}

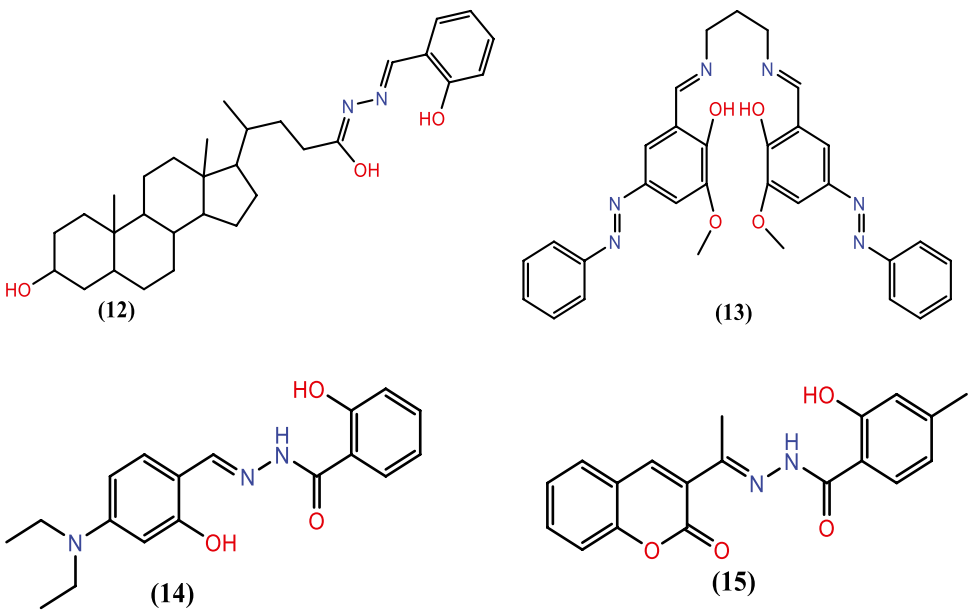

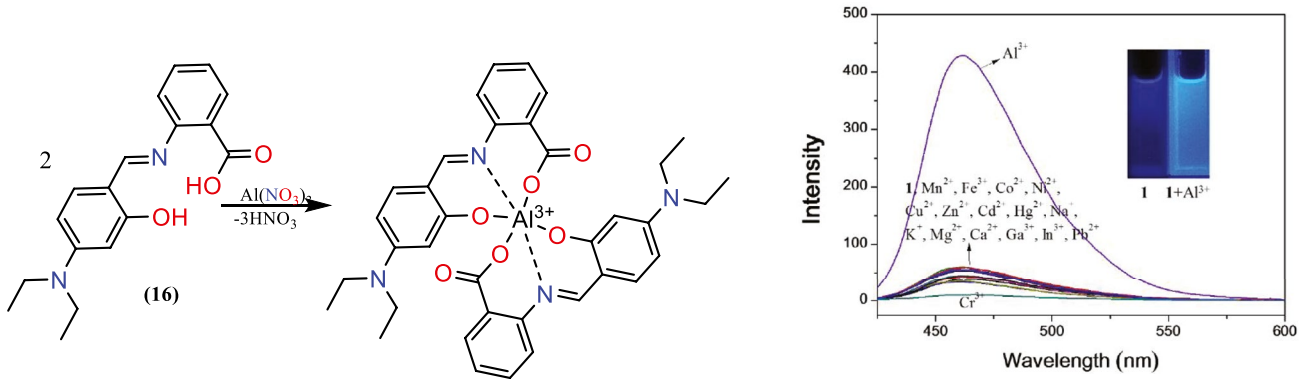

Fig. 6 **a** Proposed structure of 2:1 aluminum complex; **b** Emission spectra shown by (16)

high sensitivity towards Al^{3+} ions [85]. Initially, probe (20) exhibited negligible fluorescence, but the intensity of the emission band increased up to 5000 a.u on binding with Al^{3+}. Li et al.synthesized a diazafluorene-based Schiff base (21) by simply refluxing diazafluorene-based amine (0.175 g, 0.5 mmol) and salicylaldehyde (0.183 g, 1.5 mmol) in 70 ml methanol for 12 h [86]. The fluorescence behavior of (21) was examined towards a number of trivalent and divalent metal cations. A free form of (21) showed a poor signal of emission intensity at 475 nm when excited with the wavelength of 392 nm, whereas on adding 10 equivalents of Al^{3+} ions, a 1312-fold enhancement in fluorescence intensity was observed. Schiff base (2-((2-hydroxybenzylidene)-amino)-2-(hydroxymeth-yl) propane-1,3-diol (22) was investigated for its emission behavior towards a series of divalent (Co^{2+}, Ni^{2+}, Cu^{2+}, Zn^{2+}, Cd^{2+}, Hg^{2+}, Pb^{2+}), alkali, alkaline and trivalent (Fe^{3+}, Cr^{3+}, Ga^{3+}, In^{3+}, and Al^{3+}) metal cations in a purely aqueous medium [87]. After adding different metal cations to the solution of (22), strong enhancement was shown in the case of Al^{3+} only, along with a redshift from 405 to 459 nm. Also, under the UV lamp, the color of the solution appeared blue, which was colorless before the addition of Al^{3+}. The other characteristic parameters of ligands (17)-(22) are listed in Table 2, and the structures of these compounds are shown in Fig. 7.

Schiff base (23) was investigated for its photophysical behavior in the buffer solution of HEPES (50 mM) made in 0.01% ethanol and was effectively employed in sensing aluminum ions in human hepatocellular liver carcinoma cells [88]. This weakly fluorescent ligand showed a sharp increase in intensity at 450 nm, along with the formation of an ML_2-type complex. 10 ml ethanolic solution of $Al(NO_3)_3.9H_2O$ (0.187 g, 0.5 mmol) was added into 10 ml solution of (23) (0.241 g, one mmol) and refluxed for 2 h with proper stirring; the clear solution obtained was kept overnight, after which yellow crystals were obtained with 80% yield. Scheme 2 depicts the formation of a solid aluminum complex. Values from Job's plot and Benesi–Hildebrand expression gave the value of binding constant $K_a = 10.188 \times 10^3\ M^{-1}$. (23) was effectively employed in sensing aluminum ions in the Human hepatocellular liver carcinoma cells.

Antipyrine derivatives are of greater interest due to their pharmacological applications and clinical interest. Selvan and group reported two isomeric 4-aminoantipyrine based Schiff base ligands, (24) and (25), which recognize Al^{3+} ion in highly aqueous medium [89]. Fluorescence studies of both the probes were investigated

Table 2 Some other distinctive parameters of fluorescent sensors (17)-(22) used for the detection of Al^{3+}

Cation sensor	$\lambda_{ex}/\lambda_{em}$ (nm)	M:L ratio	Binding constant (M^{-1})	Detection limit (M)	Mechanism	Reference
(17)	278/484	1:1	2.67×10^5	1.06×10^{-7}	PET, ESIPT, CHEF (turn-on)	[82]
(18)	310/380	1:1	–	1.15×10^{-7}	ICT, PET, CHEF (off–on-off)	[83]
(19)	420/480	1:1	2.7×10^3	3.44×10^{-6}	CHEF (turn-on)	[84]
(20)	330/450	2:1	2.86×10^4	1.87×10^{-6}	CHEF (turn-on)	[85]
(21)	392/475	1:1	1.8×10^9	3.7×10^{-8}	ICT, CHEF (turn-on)	[86]
(22)	310/459	1:1	-	3.2×10^{-7}	PET, CHEF (turn-on)	[87]

Fig. 7 Structures of fluorescent chemosensors (17)-(22)

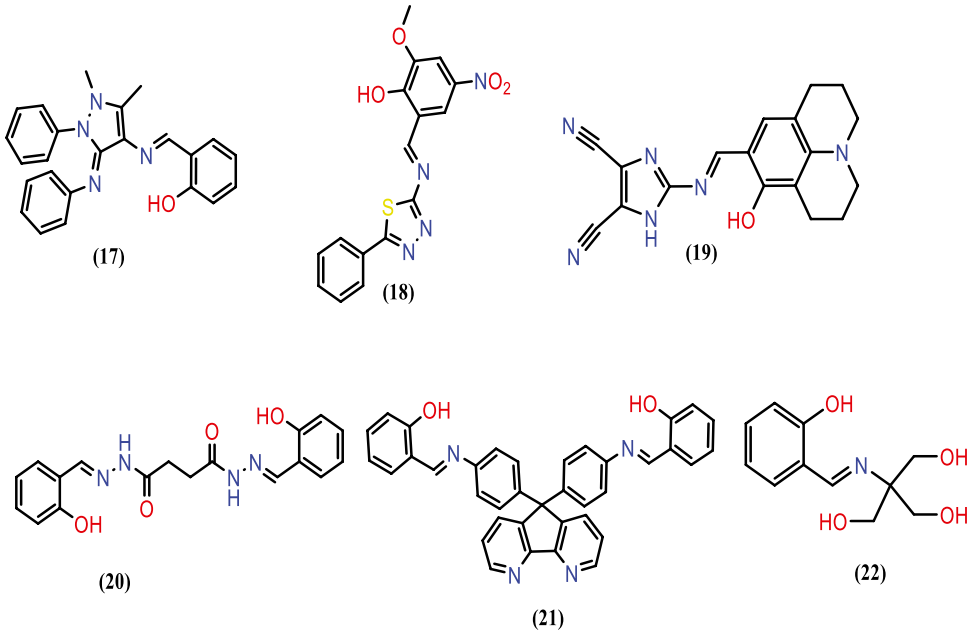

concerning different metal ions, which showed that on adding Al^{3+} to the respective solutions, 25-fold and fourfold enhancement in fluorescence intensities was observed for (24) and (25), respectively. The binding ratio of both the ligands (24) and (25) with the Al^{3+} was 1:1, as confirmed by Job's plot analysis. The binding constants evaluated are 6.02×10^{-3} M^{-1} and 5.56×10^{-3} M^{-1} for (24)–Al^{3+} and (25)–Al^{3+} complex, respectively. 2-Hydroxy naphthalene-based fluorescence sensor (26) was utilized in sensing Al^{3+} ions in larvae of living zebrafish [90]. The sensor showed no detectable fluorescence in its free form, but adding Al^{3+} to the solution of (26), showed a 150-fold increase in fluorescence intensity at 430 nm. The LOD for sensing Al^{3+} is 1.37×10^{-7} M. Sensors (24), (25), and (26) are shown in Fig. 8.

Fluorescence Sensors for Zn (II)

Zinc metal is the second most abundant d-group metal ion in the human body, which plays a vital role in various biological processes like the synthesis of DNA, neurophysiology, apoptosis, modulation of diverse ion channels, gene expression, and signal transduction. Also, Zn^{2+} is an integral part of the bio-enzymes like carbonic anhydrase, zinc finger proteins, and transcription factors. An imbalance of Zn^{2+} ions is associated with severe neurological disorders, including seizure disorder, Alzheimer's disease, Parkinson's disease, ischemic stroke, and infantile diarrhea [91–94]. Zn^{2+} metabolic disorders are also associated with hair loss, diabetes, epilepsy, etc. So, the concentration variation of Zn^{2+} should be monitored by highly selective chemosensors, and thus,

Scheme 2 Schematic representation for the synthesis of (23)-Al^{3+} complex

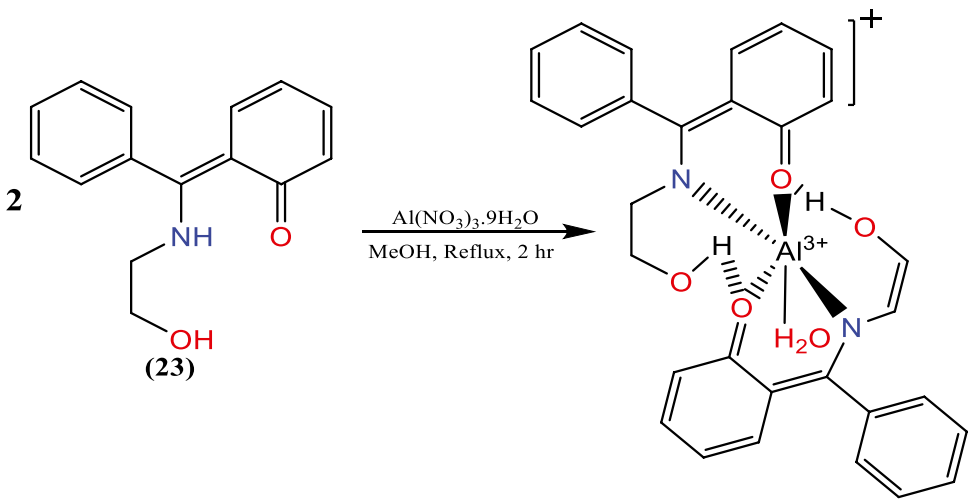

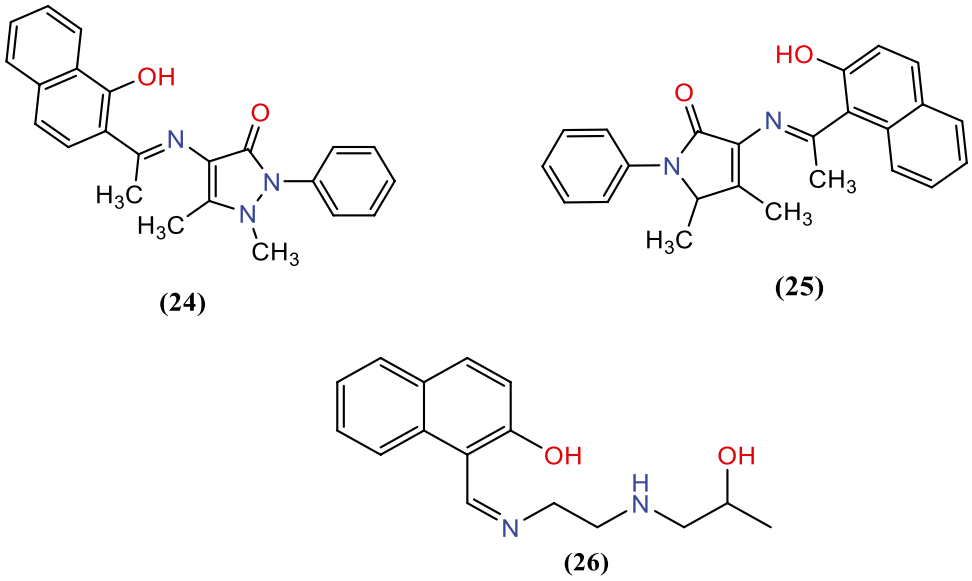

Fig. 8 Structural depiction of Aluminium sensors (24), (25) and (26)

the determination of Zn^{2+} is gaining more and more attention. A brief analysis of some Schiff base fluorescent sensors for selective determination of Zn^{2+} is examined below.

A malononitrile-based ligand (27), stable under a broad pH range, displayed an eightfold enhancement in fluorescence towards zinc ion for the peak present at 661 nm [Fig. 9a] [95]. The measured LOD value i.e., 0.44 µM, shows high sensitivity towards Zn^{2+}. The cell imaging experiments indicated that (27) could be effectively used as an assuring tool for imaging studies, thereby revealing the explicit mechanisms of Zn^{2+} in living systems. Similarly, another zinc sensor (28) showed eightfold enhancement, which could be due to the binding of (28) with Zn^{2+} ions leading to ring formation making a stable ML-type zinc complex with formation constant as 2.36×10^6 M [refer to Fig. 9b] [96]. LOD for the sensor was found to be pretty low (0.52 nM) in the pH range of 4–9. The Zn^{2+} complex of (28) has been used in live-cell imaging techniques and successfully illustrated as a feasible biomarker. The ligand and its Zn^{2+} complex were evaluated by test paper strips to assess the real-world efficacy, and the latter was also employed for the selective detection of pyrophosphate ion with the help of fluorescence mechanism.2,6-bis((*E*)-(2-(benzo[d]thiazol-2-yl)-hydrazono)methyl)-4-(4,5-diphenyl-1H-imidazol-2-yl) phen-ol(29), reported by Gomathi and the group was found to be another turn-on emission probe for zinc ions [97]. The sensing ability of (29) was tested with different metal cations in which only Zn^{2+} exhibited around an eightfold increase in intensity [Fig. 9c] with a green–blue emission band situated at 463 nm, achieving a detection limit of 10.9 µM. Stuructures of these Zinc sensors are shown in Fig. 10.

3,5-di-tert-butyl-2-hydroxybenzaldehyde and 2-hydroxybenzaldehyde were reacted with amino acid l-glutamine to produce Schiff bases (30) (yellow solid) and (31) (yellow oil) with 56% and 77% yield respectively when refluxed for 24 h in methanol solution [98]. These

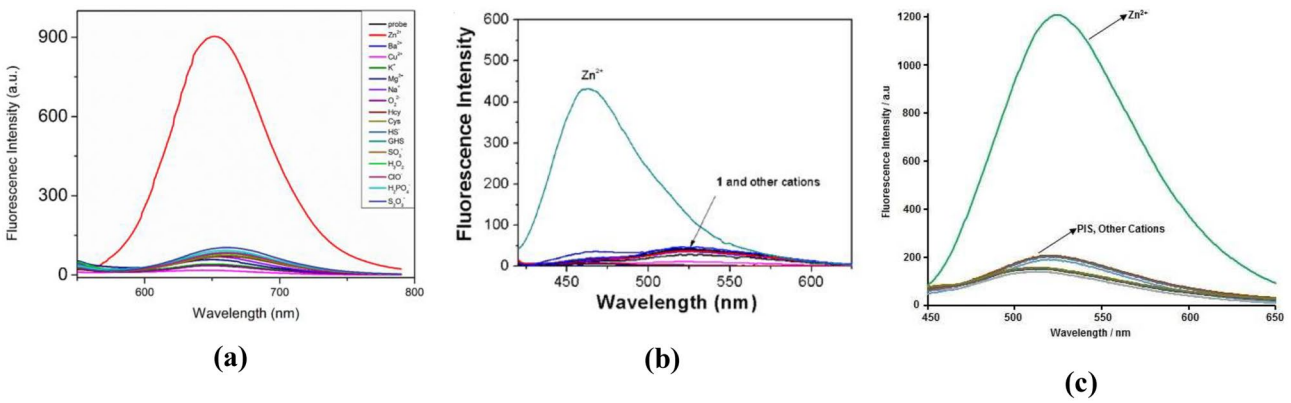

Fig. 9 Emission behavior of ligands (a) (27), (b) (28), (c) (29) in the presence of metal ions

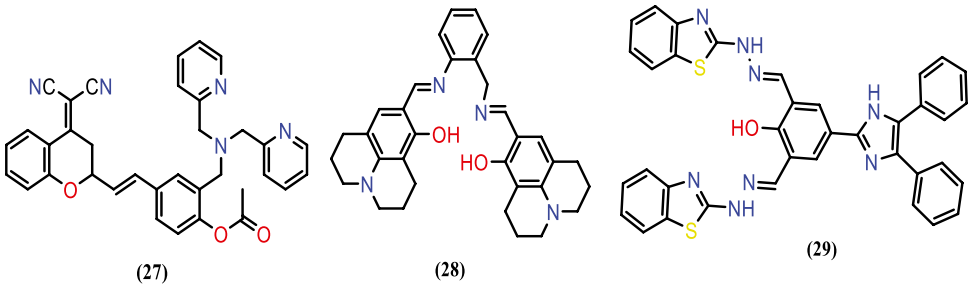

Fig. 10 Zinc sensors (27), (28), and (29)

sensors were documented for selective detection of zinc ions in acetonitrile–water (1:1) as a medium, having LOD values of 1.17 and 1.20 mM, respectively. The ligand was also used to determine intracellular zinc ions in the human epithelial cells via the live cell imaging process. The photophysical studies of (30) revealed a weak emission band exhibition at 475 and (31) at 445 nm on excitation at 370 nm. The DFT studies revealed that electron transfer taking place from HOMO to HOMO-1 results in the poor emission of free sensors. Upon binding with Zn^{2+}, both molecules showed up to a 30-fold enhancement in the fluorescence intensities. This increase in fluorescence can be explained due to the restriction of PET and structural rigidity after complexing with Zn^{2+} ions (Fig. 11).

Low-level recognition of Zn^{2+} ions can also be done using diarylethene derivative-based Schiff base (32) in THF solvent, which on excitation at 380 nm, produces a weak emission band at 464 nm [99]. Upon addition of a stock solution of different metal cations one by one, (32) shows a 27-fold enhancement in fluorescence intensity only for Zn^{2+}ion along with a red shift (464 to 513 nm) and color change from blue to bright green. This behavior of the sensor is due to the formation of the complex (ML type) [Fig. 12], for which isomerization of C = N bond was suppressed, and CHEF came into the picture.

Zinc sensors (33)–(38) are shown in Fig. 13, along with their binding parameters listed in Table 3. The fluorescence behavior of a quinoline-based reversible chemosensor (33) was investigated in a 1:1 acetonitrile: water medium, which was found to be weakly fluorescing [100]. Upon gradual addition of Zn^{2+} ions to the ligand solution, a 53-fold increment in fluorescence was observed. Along with sensing Zn^{2+} ions in the human cervical cancer cells, this sensor was also helpful in building an "INHIBIT" type logic gate with Zn^{2+} ions and EDTA as inputs. Studies of a guanidine-based Schiff base (34) in CH_3OH-tris buffer solution resulted in weak fluorescence emission at 585 nm when excited at 395 nm. In contrast, emission intensity increased almost 25-fold in the presence of Zn^{2+}[101]. Kim and co-workers developed another zinc sensor (35), which was effectively used in the imaging studies of zinc ions in living Hela cells [102]. Emission studies of (35) were done in a purely aqueous medium. Receptor (35) displayed a weak emission band (intensity 45 a.u approx.) at 479 nm, but with Zn^{2+}, this intensity increased to 200 a.u. An orange solid Probe (36) showing a parent peak in ESI-Mass at 565.32 was derived through the condensation process of 3,3'-Diaminobenzidine (100 mg, 0.46 mmol) and 4-(N,N-diethyl)-2-hydroxybenzaldehyde (181 mg, 0.93 mmol) in ethanol, when refluxed for 3 h [103]. Studying the fluorescence behavior proved to be a dominatingly selective sensor towards Zn^{2+} ion (54-fold enhancement). The LOD value was as low as 8.6×10^{-9} M for Zn^{2+}, indicating its high efficiency in detecting a nanomolar concentration of Zn^{2+}, thereby imparting potential application in the selective detection of zinc in environmental samples. A 4,5-diazafluorene-based molecule (37) showed selectivity towards Zn^{2+} by displaying a 194-times increase in fluorescence at 465 nm, which is due to the complex formation because on complexing with the zinc metal ion, the hydroxyl proton is removed, which results in the restriction of ESIPT mechanism and thereby increasing the fluorescence [104]. A pyridine-based Schiff base (38) was prepared by adhering it to the surface of organically modified SBA-15 mesoporous silica [105]. The fluorescence

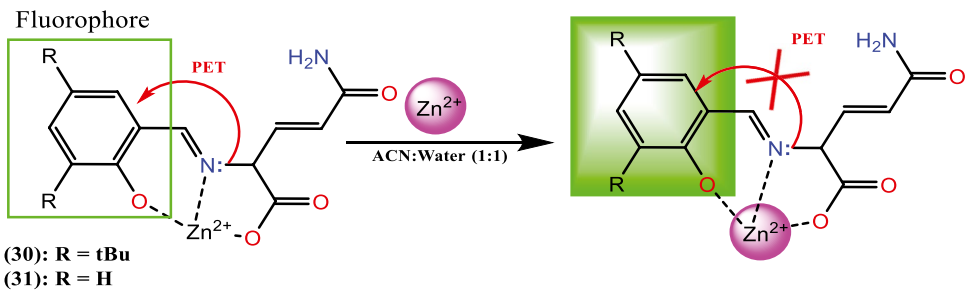

Fig. 11 Fluorescence enhancement mechanism of (30) and (31) involving PET-blocking process

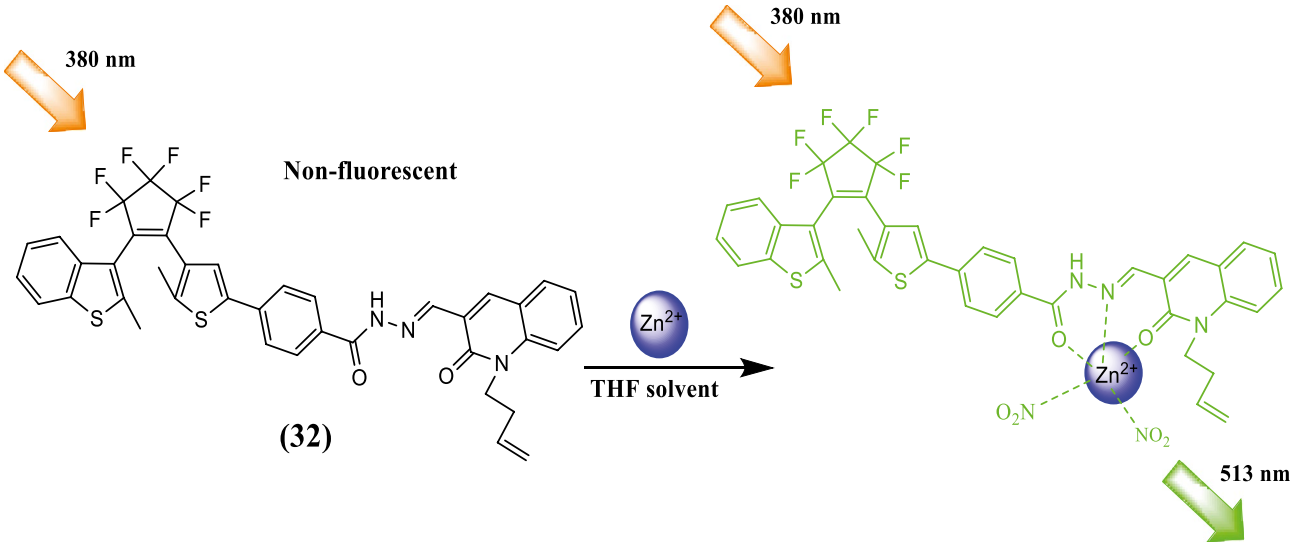

Fig. 12 Formation of (32)-Zn^{2+} complex during fluorescence studies

performance of this sensor towards Zn^{2+} was recorded in a purely aqueous medium. The molecule (38) alone displayed a strong emission band at 400 nm on excitation with 300 nm wavelength. Upon addition of Zn^{2+} to it, drastic enhancement in emission intensity (200–650 a.u) was seen, which was not present in the case of any other metal ion as a result of the spectrofluorometric titrations.

A series of Schiff bases (41), (42), (43), and (44) were prepared by refluxing of 4,4′-diaminodiphenylmethane (39) for 12 h in methanol with salicylaldehyde, o-vanillin, 2,4-dihydroxybenzaldehyde and 4-formylbenzoic acid respectively [Scheme 3] [106]. All four compounds having high yields were characterized by IR, NMR, and mass spectroscopies. After adding Zn^{2+}, the fluorescence properties of the four probes, as mentioned earlier, revealed that (41) ($\lambda_{ex}=391$ nm, $\lambda_{em}=489$ nm), (42) ($\lambda_{ex}=285$ nm, $\lambda_{em}=460$ nm) and (43) ($\lambda_{ex}=372$ nm, $\lambda_{em}=530$ nm) with the electron-donating group enhanced the fluorescence intensity by 97-fold, 18-fold, and 60-fold respectively. In comparison, (44) ($\lambda_{ex}=273$ nm, $\lambda_{em}=352$ nm) with the electron-withdrawing group quenched the emission intensity up to tenfold only in the case of the Zn^{2+} ion.

Hydrazone-based Schiff-base fluorescent sensor (47) was synthesized by reacting (45) (0.102 g, 0.5 mmol) and (46) (0.101 g, 0.5 mmol) in ethanol with a yield of 71.4% [Scheme 4] [107]. The molecule showed high selectivity

Fig. 13 Structures of Schiff bases (33)-(38)

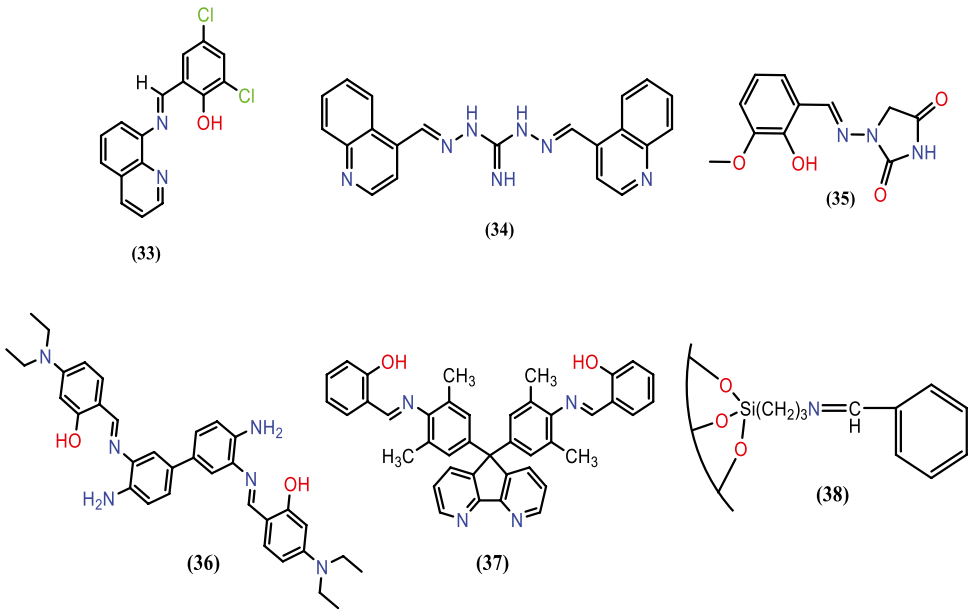

Table 3 Binding parameters of Zinc sensors (33)-(38)

Cation sensor	$\lambda_{ex}/\lambda_{em}$ (nm)	M:L ratio	Binding constant (M^{-1})	Detection limit (M)	Mechanism	Reference
(33)	355/553	1:1	3.21×10^{6}	5.0×10^{-9}	CHEF (off–on-off)	[100]
(34)	395/585	1:1	8.71×10^{3}	2.04×10^{-6}	PET, CHEF (turn-on)	[101]
(35)	380/479	1:1	4.5×10^{3}	11.9×10^{-6}	CHEF (turn-on)	[102]
(36)	430/509	2:1	7.8×10^{4}	8.6×10^{-9}	C=N, CHEF (turn-on)	[103]
(37)	465/394	2:1	2.5×10^{3}	5 ppm	ESIPT,CHEF (turn-on)	[104]
(38)	300/400	1:1	-	-	PET, CHEF (turn-on)	[105]

for the zinc ions by establishing a strong elevation in the intensity (20 a.u to 250 a.u) of the emission peak at 498 nm, forming ML type complex in the solution. The LOD calculated for Zn^{2+} is 1.73×10^{-7} M.

Another work provides a design strategy for constructing six new Schiff base fluorescent probes [108]. The fluorescence properties of these target probes (48), (49), (50), and reference probes (51), (52), and (53) [Fig. 14] interpreted that only the target probes exhibited significant elevation in the intensity of emission spectra in the presence of Zn^{2+} whereas, the reference probes showed no change in the fluorescence spectra. The fluorescence spectra of the target probes (48), (49), and (50) displayed two emission bands; the first band at around 400 nm, and the second band concerning the first band is present with redshift at 169 nm in case of (48) and 171 nm in case of (49) in ethanol medium. Further, on adding different metal ions to the respective target probes, an elevation in fluorescence intensity was observed in the presence of Zn^{2+} only. Probe (49) displayed a 40 times increment in the fluorescence with a new peak at 500 nm with Zn^{2+}, and the signal due to ESIPT at 530 nm disappeared. A 35-fold enhancement was noticed for (48) and (50). The association constants (K_a) of all three complexes with stoichiometric ratio 1:1 were calculated as 1.37×10^{6} M^{-1} (48), 1.42 10^{6} M^{-1} (49), and 1.13 10^{6} M^{-1} (50), respectively. Moreover, these chemical sensors showed promising results on a broader pH range thus, can be efficiently used in live-cell imaging of zinc ions with considerable fluorescence variation.

Fluorescence Sensors for Cu (II)

Copper is a renowned trace metal for the proper functioning of the human body as it participates in several cellular processes and metabolic functions. It is an indispensable metal for humans, plants, and animals. Copper is involved in metabolic processes like enzymatic hydrolysis, generation and regulation of nerve signals, electron transfer, energy production, and formation of bones, and it also acts as an effective catalyst in various redox processes. Everyday consumption of copper should be 1.2–1.3 mg/day as per WHO. When the concentration of Cu^{2+} crosses the limit, it causes diseases like prion disease, Alzheimer's disease, and Wilson's disease [109–113].

An organic–inorganic hybrid nanosensor (54) was developed from a bis-salicylaldehyde-based Schiff base and SBA-15 mesoporous silica [114]. The aqueous suspension of (54) showed a strong fluorescence emission band at 435 nm ($\lambda_{ex}=317$ nm), and the fluorescence quenched dramatically only in the presence of copper metal ion [Fig. 15a] with a limit of detection as 8.4 10^{-3} mg/L. The quenching in emission intensity is due to the formation of a coordination complex between the ligand and Cu^{2+} ion through the electron-donating phenolic hydroxyl groups and the nitrogen atom. The paramagnetic nature of the Cu^{2+} ion is also responsible for the quenching. Regeneration studies of this compound were performed using Na_2-EDTA (acting as a

Scheme 3 Synthesis scheme for probes (41), (42), (43), and (44)

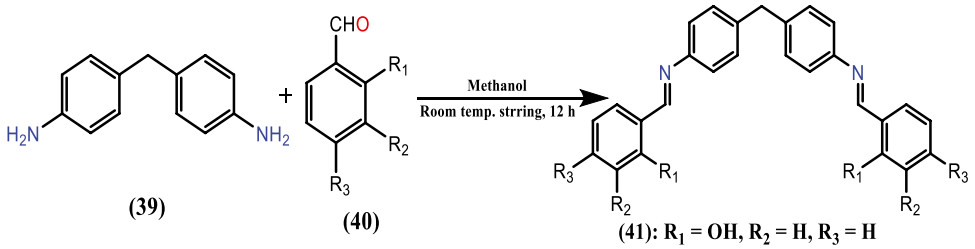

(41): R_1 = OH, R_2 = H, R_3 = H
(42): R_1 = OH, R_2 = H, R_3 = OH
(43): R_1 = OH, R_2 = OCH_3, R_3 = H
(44): R_1 = H, R_2 = H, R_3 = COOH

Scheme 4 Synthesis of Schiff base (47)

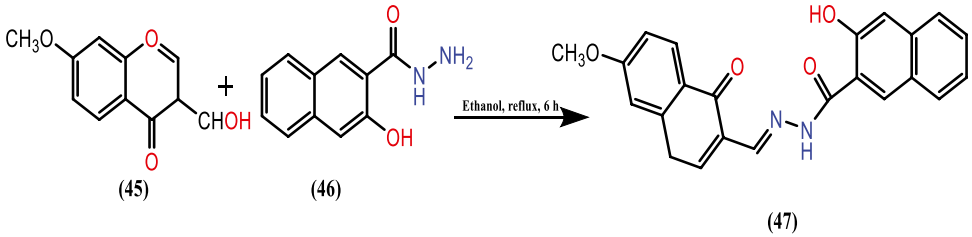

desorption agent) solution, which recovers the nanosensor (54) from its copper complex. Hence it can be utilized again and again for practical purposes. Another Schiff base (55) was derived from p-toluic hydrazide and 4-tert-butyl-2,6-diformyl phenol, which was found to be a colorimetric as well as a fluorometric sensor in the ethanolic medium [115]. The fluorescence performance of this ligand showed a decrement in the fluorescence intensity from 600–20 a.u in the presence of Cu^{2+} ion [Fig. 15b]. This can be explained on the basis of the reverse PET mechanism occurring from the N, O atoms of carbohydrazide moiety to the OH of the phenol group in (55), leading to the formation of a dinuclear dimeric copper complex. A hydrophilic Schiff base (56) was incubated in the HeLa cells. On irradiating the loaded HeLa cells with UV light, bright green-colored fluorescence was seen at 37 °C [116]. Further addition of copper ion to the above system quenched the fluorescence. Regeneration studies of probe (56) having $\lambda ex = 436$ nm and $\lambda_{em} = 532$ nm were done with Na_2EDTA solution. The studies explored the chemosensor as reproducible and could be used repeatedly for sensing Cu^{2+} ions at low concentration levels ($LOD = 3.74 \times 10^{-8}$ M^{-1}) in water. The fluorescence spectra of (56) in the presence of several cations are shown in Fig. 15c. Figure 16 represents the structures of the above-discussed Schiff bases (54), (55), and (56).

The molecule (57) behaves as a colorimetric and fluorometric chemosensor and shows a strong emission band at 519 nm in the physiological pH (7.4). The Schiff base (57) showed 2.5-fold quenching in the fluorescence on complexing with Cu^{2+} due to the Dexter-type electron transfer from Cu (II) center to the photoexcited fluorophore. A color change was observed from light pink to yellow due to the complex formation between (57) and Cu^{2+} ions [Fig. 17] [117].

2-Hydroxy-1-napthaldehyde (58) in reaction with benzylamine (59) in methanol solution gave rod-shaped crystals of Schiff base (60) with a yield of 80%, as shown in Scheme 5 [118]. Single crystal XRD confirms the structure of the sensor, and the fluorescence behavior studies revealed its high selectivity towards copper ion in DMSO: H_2O (2:8) system. The poor fluorescent molecule ($\lambda_{ex} = 320$ nm and

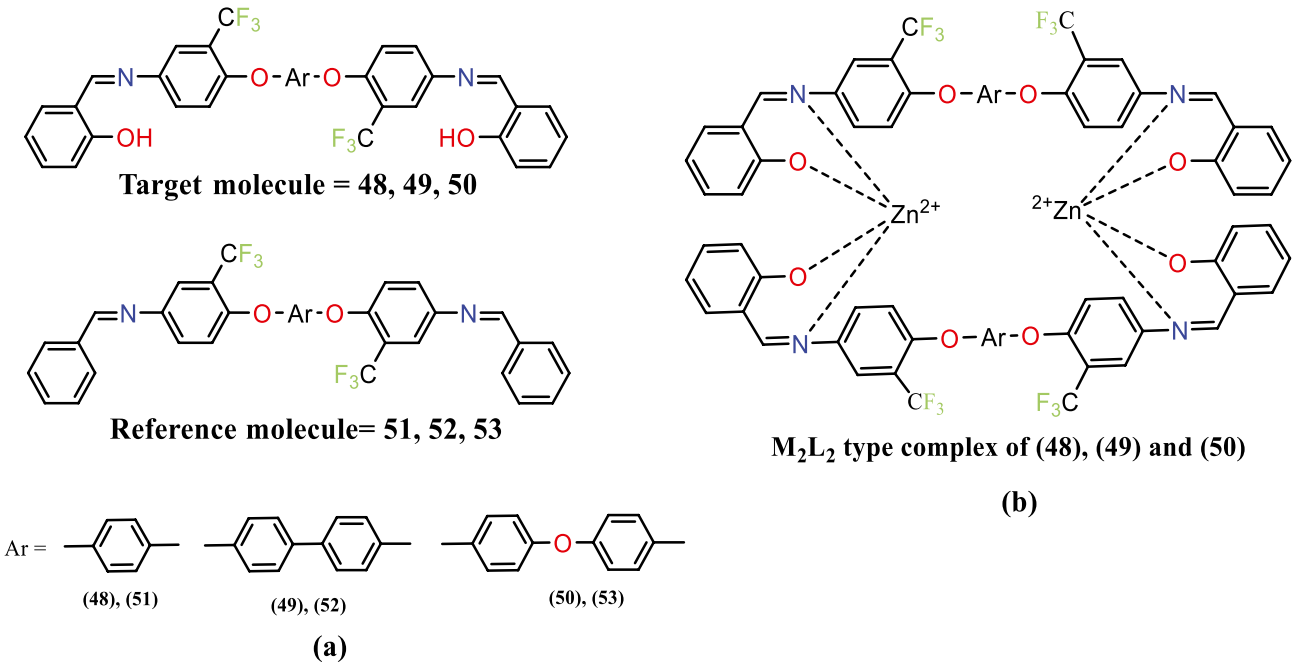

Fig. 14 **a** Structures of the sensors (48), (49), and (50) correspond to the target molecule, while 51, 52, and 53 relate to reference probes; **b** Complex of sensors (48), (49), and (50) with Zn^{2+}

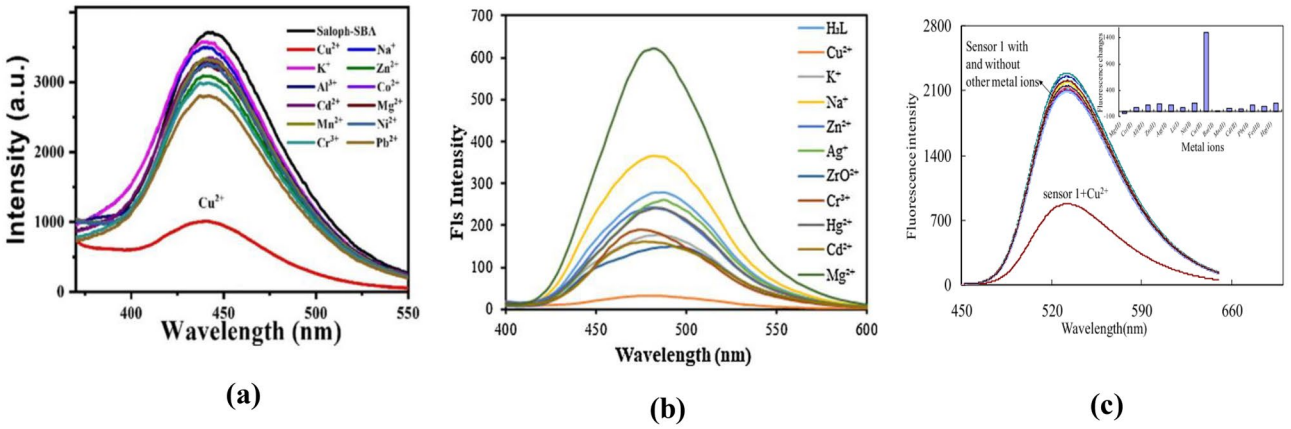

Fig. 15 Emission spectra of **a**-(54), **b**-(55) and **c**-(56)

$\lambda_{em} = 645$ nm) is a turn-on fluorescence sensor for the copper metal ion, which could be explained by the restriction of the ICT mechanism (occurring in the naphthalene moiety), resulting in the formation of rigid ML_2 type Cu-complex. The value of the association constant and detection limit for the copper complex were reported as 1×10^{11} M^{-2} and 30×10^{-9} M, respectively.

A few other copper sensors (61)-(68) discussed here are represented in Fig. 18, along with their characteristic properties listed in Table 4. Detection of the copper ion at the micromolar levels in the biological and water samples was achieved using the sensor (61), having a low detection limit of 0.36 µM [119]. Fluorescence studies of the above-mentioned sensor done in THF-water solvent displayed quenching in fluorescence at 565 nm, in the presence of copper ion forming a highly stable copper complex. Similar synthetic pathways were followed by Kowser et al. to produce two new fluorogenic molecules (62) and (63) [120]. Both the reported molecules were weakly fluorescent due to the electron transfer process occurring from the nitrogen atoms to the pyrenyl fluorophore of each sensor independently. While performing the sensing studies, copper complexes of (62) and (63) formed in solution blocked the electron transfer process, resulting in an increase in fluorescent intensity by 65-fold and 25-fold for (62) and (63), respectively. The condensation of N-(3-Aminopropyl)imidazole and 2-Hydroxy-5-(ptolyldiazenyl)-benzaldehyde resulted in orange colored Cu^{2+} sensor (64) with 82% yield, which was characterized by single crystal XRD [121]. The molecule displayed a 50-fold enhancement in the intensity

Fig. 16 Cu^{2+} sensing Schiff bases- (54), (55), and (56)

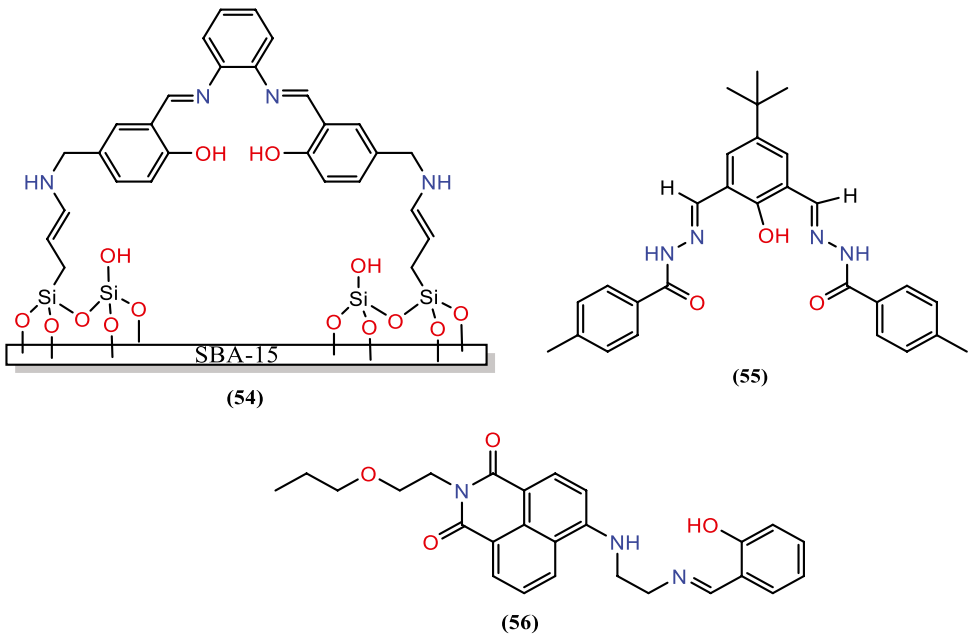

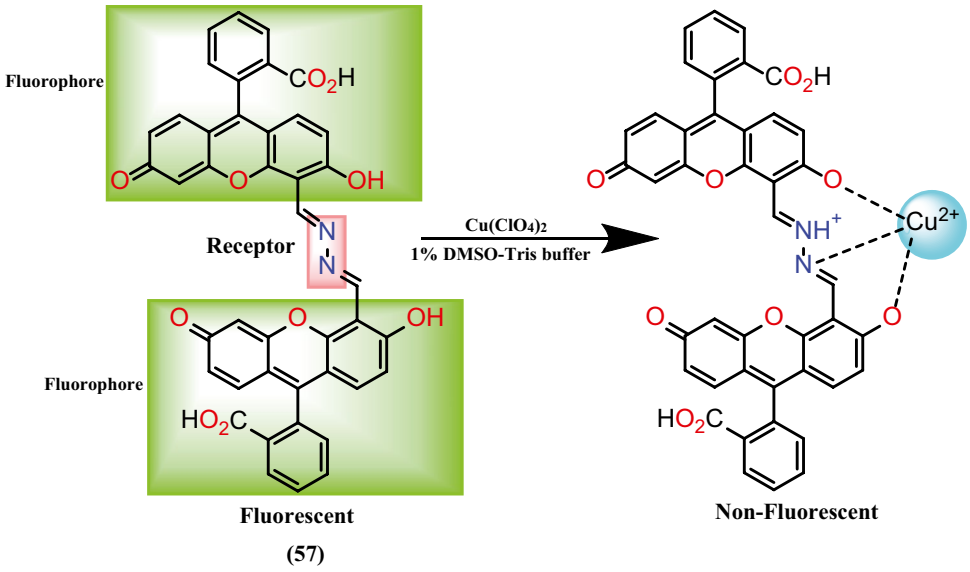

Fig. 17 Sensing mechanism of Schiff base (57) towards copper ion

with Cu^{2+} ion. The combined effect of CHEF and restriction in cis–trans isomerization were responsible for this increment. Upon the gradual addition of copper ions into the solution of a new naphthalene-based Schiff base derivative (65), an enhancement in emission intensity from 50 a.u to 550 a.u was observed, which was absent in the case of other metal ions [122]. Pyrene-based carbaldehyde and carbonohydrazide amine were refluxed in an ethanol medium to produce Schiff base (66), which selectively recognizes the biologically important Cu^{2+} in semi-aqueous suspension [123]. This molecule initially showed a weak band in the emission spectra, but after adding Cu^{2+}, a 4.5-times elevation was observed at 455 nm. This ligand was effectively used in governing the intracellular copper ion in HeLa cells. The photophysical properties of a naphthalimide-based Schiff base (67) were studied through excitation and emission spectroscopy in a tris–HCl buffer-DMF solution [124]. A significant quenching in fluorescence intensity (from 980 to 320 a.u approximately) was noted at 539 nm only in the presence of Cu^{2+} ions. The test strips of a Schiff base (68) were fabricated to investigate its practical applications [125]. This molecule depicted 95-fold quenching in the fluorescence band present at 520 nm, along with a notable color change from yellow to colorless in the presence of Cu^{2+} ions.

Fluorescence Sensors for Ag(I)

Silver is one of the precious metals and has a wide variety of applications in the industries like pharmacology, photography, medicine, jewelry, electronics, etc.. Besides that, silver is also used as an antimicrobial agent in silver-impregnated filters for water purification. These widespread applications have resulted in the accumulation of silver in the environmental systems. 0.2 µM concentration of Ag^+ is allowed for the human body. A concentration of more than this can cause severe damage to the human body [126–131]. So, there is a need for effective sensing of silver species in the waste-water samples. Sahu and the group developed the pyridine-based Schiff base (69), which recognizes silver ina methanol–water (1:1) binary solvent mixture [132]. Sensor (69) is a feebly emitting molecule showing an emission band at 416 nm ($\lambda_{ex} = 330$ nm). After adding different metal cations (Fe^{2+}, Co^{2+}, Cu^{2+}, Ni^{2+}, Zn^{2+}, Cd^{2+}, Hg^{2+}, Pb^{2+}, Cr^{3+}, Al^{3+}, Fe^{3+}, and Ag^+ ions), only in the case of Ag^+ drastic enhancement (~ 25-fold) in fluorescence was observed at 416 nm along with a noticeable change in color from colorless to deep-blue forming an M_2L type complex in solution. This molecule binds with one silver ion through the 'N'-atom of

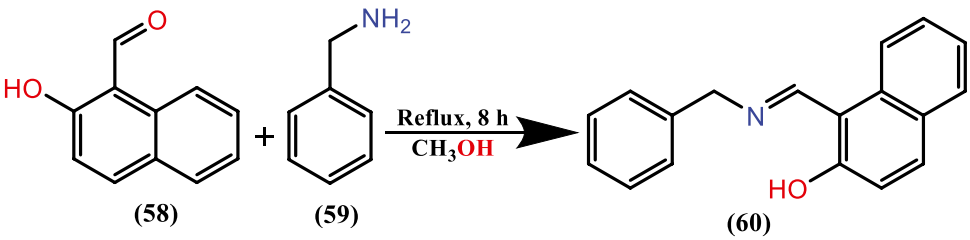

Scheme 5 Synthesis scheme for the preparation of Schiff base (60)

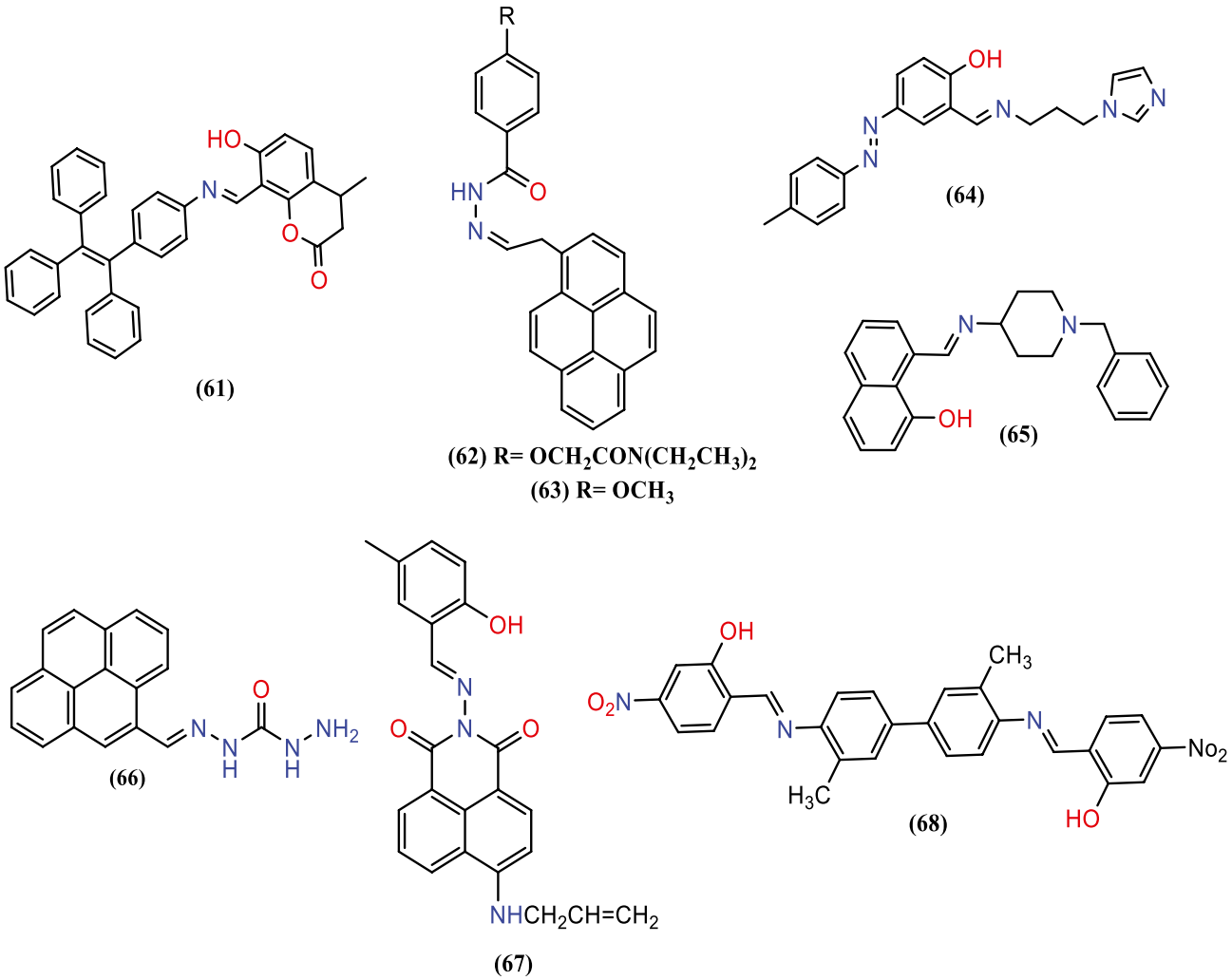

Fig. 18 Representation of copper sensors (61)-(68)

pyridine fluorophore, along with one nitro group and two water molecules, whereas another silver atom bind with (69) through 'N' and 'S' atoms of thiourea group along with two water molecules leading to the formation of stable dimeric complex [Fig. 19].

Fluorescence Sensor for Cd(II)

Cadmium is a silvery-white, soft metal belonging to group 12 of transition metal atoms. Cadmium reassembles mercury and zinc metal in most of its properties. Amongst the

Table 4 Characteristics of Copper sensors (61)-(68)

Cation sensor	$\lambda_{ex}/\lambda_{em}$ (nm)	M:L ratio	Binding constant	Detection limit (M)	Mechanism	Reference
(61)	365/565	1:2	-	0.36×10^{-6}	CHEQ (turn-off)	[119]
(62)	367/405	1:1	1.29×10^{5} M^{-1}	8.80×10^{-8}	PET, CHEF (turn-on)	[120]
(63)	367/405	1:1	1.55×10^{4} M^{-1}	4.94×10^{-7}	PET, CHEF (turn-on)	[120]
(64)	385/426	1:2	-	1.8×10^{-6}	C = N, CHEF (turn-on)	[121]
(65)	234/345	1:1	4×10^{4} M^{-1}	-	CHEF (turn-on)	[122]
(66)	370/455	1:2	1.89×10^{9} M^{-2}	3.5×10^{-8}	CHEF (turn-on)	[123]
(67)	430/539	1:1	1.32×10^{6} M^{-1}	2.3×10^{-5}	CHEQ (turn-off)	[124]
(68)	375/520	2:1	6.1×10^{10} M^{-2}	4.87×10^{-9}	CHEQ (turn-off)	[125]

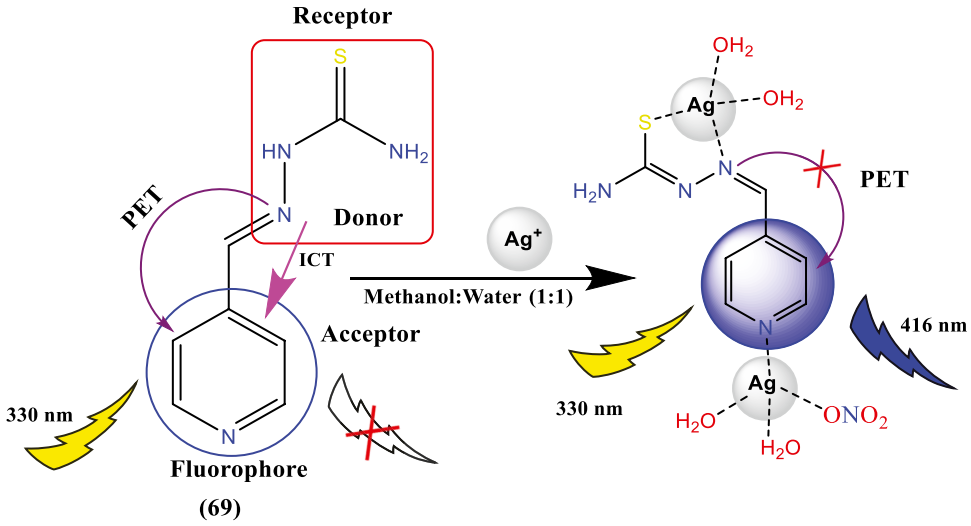

Fig. 19 Plausible sensing mechanism of (69) for Ag^+

other heavy metal ions, cadmium is one of the most toxic. Excessive exposure to cadmium may lead to renal dysfunction, forms various types of cancers, and can collapse the metabolic calcium rate. Higher concentrations of cadmium released into the environment from industries may contaminate the soil, water, and crops, harming aquatic life and human health. As Cd^{2+} behaves like Zn^{2+}, it can replace zinc from the zinc enzymes and will lead to dis-functioning those enzymes. That is why explicit recognition of this toxic metal is essential [133–135].

Schiff base (72) was produced with (79% yield) by stirring of 2-hydroxy-napthaldehyde (0.2 g, 1.1 mM) (70) with 2-hydrazinoquinoline (0.185, 1.1 mM) (71) in slightly acidic methanol medium for half hour at room temperature. The formation of (72) was confirmed by the presence of parent peak in HRMS data 314.1288, IR, and NMR data [Scheme 6] [136]. Treatment of Cd^{2+} with (72) in an acetonitrile–water (8:2) medium forms a rigid complex, binding through -OH (of quinolone) and N (of imine), restricting C = N isomerization ultimately. The emission bands initially at 330 nm and 380 nm exhibited a bathochromic shift to 436 nm and 456 nm, showing a 37-fold enhancement. A visible color change from colorless to crimson yellow was seen immediately after adding Cd^{2+} to the stock solution of the sensor. The DFT studies confirmed the reduction in band gap energy (4.13 eV—2.86 eV) from the compound (72) to its cadmium complex, which is also attributed to its good fluorescence response. The ligand (72) was used successfully to evaluate cadmium concentration in various water samples.

A Naphthalene-based sensor (75), with 87.93% yield, was prepared by refluxing 2-hydroxynapthaldehyde (200 mg, 1.10 mmol) (73) and 2-hydrazinobenzothiazole (190 mg, 1.10 mmol) (74) for 3 h [Scheme 7] [137]. (75) was reported to sense cadmium ions. The spectrofluorometric studies of (75) in a DMSO-water mixture displayed a weak fluorescence band at 507 nm. After adding Cd^{2+}, a nine-fold enhancement in intensity and the hypsochromic shift from 507 to 497 nm were noted. The value of the association constant for the M:L type complex was $1.17 \times 10^4\ M^{-1}$. The imaging experiments checked the practicability of this probe. HeLa cells loaded with (75) showed minimum fluorescence, while on treating the above cells with Cd^{2+} for 10 min, bright fluorescence was noted.

Fluorescence Sensors for Cr(III)

Chromium is commonly found in the earth's crust in Cr^{3+} and Cr^{6+} oxidation states. Cr^{6+} is highly toxic, whereas Cr^{3+} is essential for human nutrition. Cr^{3+} plays a vital role in activating certain enzymes, which are also required in the catabolism of proteins, carbohydrates, fats, and nucleic acids. Although, excess and insufficiency of chromium will lead to several health diseases, such as diabetes and heart problems, which impact cellular structure and normal enzymatic activities. The environmental protection agency (EPA)

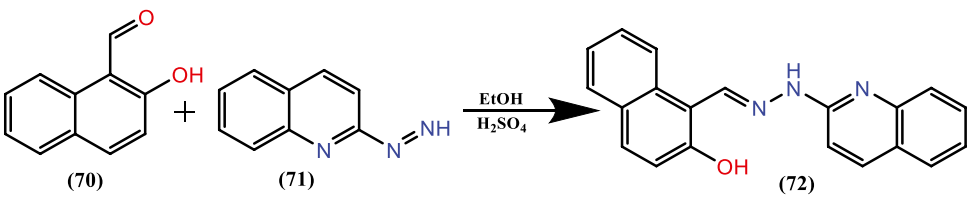

Scheme 6 Synthesis scheme of chemosensor (72)

Scheme 7 Synthesis scheme of probe (75)

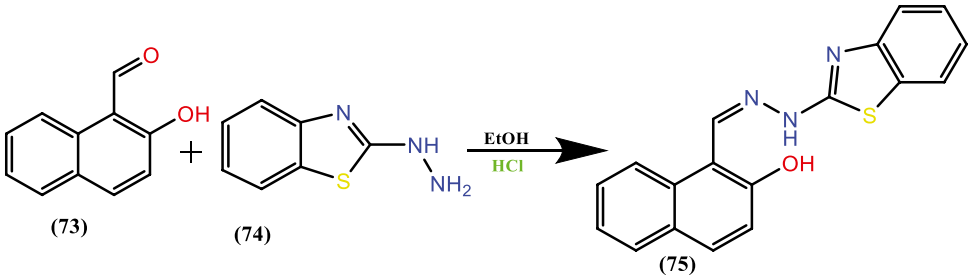

sets the maximum permissible limit of total chromium as 0.1 mg/mL [138–142]. So, the detection of Cr^{3+} is essential. Chalmardi et al. developed two chemosensors (76) and (77) only by differing the binding position of 'N' atoms in the moiety [Fig. 20] [143, 144]. Emission studies of both probes were done in an acetonitrile–water medium (95/5%), which revealed that molecules (76) and (77) were negligibly fluorescent. However, they displayed considerable elevation (~ 100-fold) and (~ 70-fold) in the fluorescence with Cr^{3+}, respectively, and formed ML-type stable metal-chelate in solution. The LOD values calculated for (76) and (77) are 2.2×10^{-7} M, 1.3×10^{-7} M, and formation constants values are 8.77×10^{4} M^{-1}, 2.28×10^{5} M^{-1}, respectively.

Fluorescence Sensors for Fe(III)

Iron is one of the key elements in the human body required to fulfill the normal physiological functioning of the body. Iron involves several cell processes, counting DNA and RNA synthesis, oxygen transport, and energy production [145, 146]. Nonetheless, the deficiency or excess of iron leads to many diseases, such as liver damage, kidney failure, anemia, cancer, Alzheimer's, and Parkinson's diseases, and also causes lipid peroxidation and DNA fragmentation leading to cell death. [147, 148]. Iron exists in two forms: ferrous ion (Fe^{2+}) and ferric ion (Fe^{3+}). Fe^{3+} is the less reactive form due to its better water solubility, good binding affinity, and intracellular reductive environment

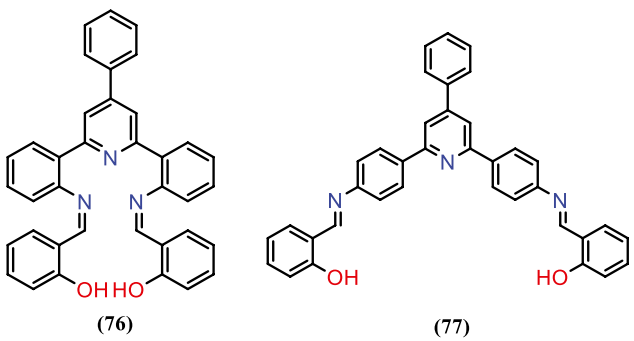

Fig. 20 Structural representation of Cr^{3+} sensors (76) and (77)

[149–151]. Some examples of Schiff bases, which selectively recognize Fe^{3+}, are discussed below.

Li and the group produced a Schiff base containing an acyl hydrazone moiety (78), which showed exciting fluorescence properties in a methanol solvent system [152]. In the presence of Fe^{3+}, molecule (78) showed 69-fold quenching at 506 nm. Emission intensity decrement was due to the paramagnetic nature of Fe^{3+} and the breaking of the H-bond between the proton of -CO–NH- and oxygen of the C = O group. For the practical applicability of the sensor (78), the authors have developed its test strips by soaking strips of Whatman filter paper into the methanolic solution of the molecule (78) for Fe^{3+} sensing. Also, the probe is applied to measure the concentration of Fe^{3+} in different water samples such as tap water, water from rivers etc. Another sensor (79) for Fe^{3+} sensing showed off–on type fluorescence behavior in CH_3OH/H_2O (9:1) [153]. This feebly fluorescent Schiff base (having intensity 90 a.u) on binding with Fe^{3+} imparted slight enhancement in fluorescence up to 130 a.u. So, (79) can effectively determine the concentration of Fe^{3+} in environmental and biological samples. A highly fluorescent sensor (80) having emission intensity ~ 1000 a.u and $\lambda_{ex} = 280$ nm showed two emission peaks between 330–520 nm, one at 356 nm and another at 372 nm [154]. The high fluorescence of (80) was due to two carbazole moieties suspended on both ends of the diaminomalonitrile group in the ligand, which forms a highly conjugated system. The binding interaction of (80) was studied with different metal cations; in the case of Fe^{3+}, fluorescence intensity was quenched from 5000 a. u to 2000 a.u in DMF. The probe (81) showed good fluorescence when bombarded with a light source having 425 nm wavelength, but this fluorescence was quenched up to ninefold in the presence of Fe^{3+} [155]. The naked-eye studies of Schiff base (81) revealed its colorimetric sensing behavior on complexing with Fe^{3+} species, i.e., yellow to colorless. Figure 21 depicts the structures of Schiff bases (78)-(81), and other parameters of these probes are discussed in Table 5.

Four iron sensors (78), (79), (80), and (81) have been prepared by refluxing the amines and aldehydes in ethanolic medium, producing a yield of 82%, 76%, 10%, and 88.25%, respectively. All four compounds were

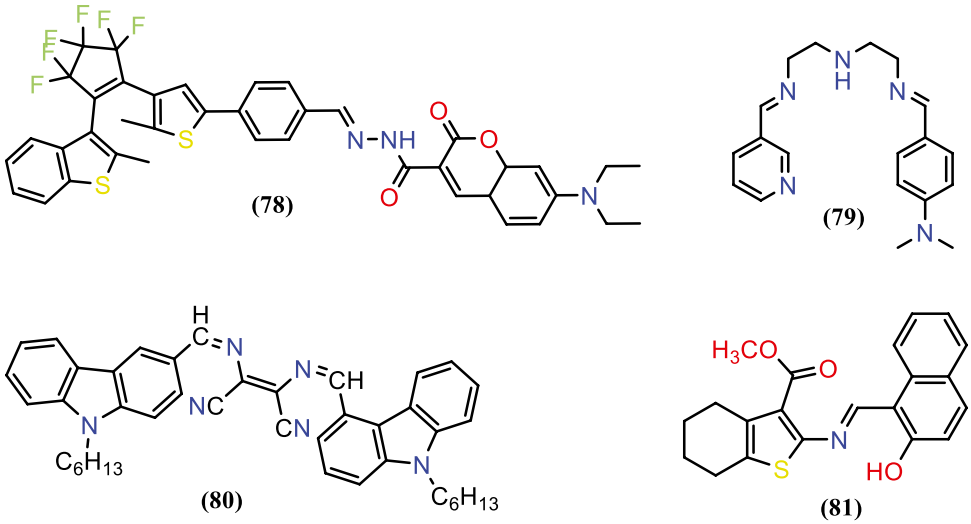

Fig. 21 Structures of Fe^{3+} sensing probes

characterized by IR, ^{1}H, ^{13}C NMR, and mass techniques [132–135].

Fluorescence Sensors for Hg (II)

Mercury, amongst various heavy metal ions, is one of the most harmful elements commonly found in air, water, and soil and is a non-radioactive heavy metal ion. Mercury is an exceedingly dangerous and universal pollutant causing severe damage to human health. According to WHO's recommendation, the maximum limit of Hg^{2+} in drinking water is two ppb [156–158]. Further, it is challenging to degrade and can cause serious harm to the central nervous system. The aggregation of mercury in the body of human beings leads to several health diseases, such as Minamata disease and various cognitive and mortar disorders. It can damage the human heart, stomach, kidneys, and genes [156, 159, 160]. So, there is a high demand for mercury sensors. A few of them are discussed below.

A thiocarbohydrazide Schiff base (82) behaves as a chemosensor for Hg^{2+} ions in a semi-aqueous medium [161]. Solution studies of (82) suggest the formation of a 1:1 mercury complex, followed by quenching of the emission intensity. This change may be due to the combined CHEQ and PET mechanisms [Fig. 22]. The limit of detection and association constant calculated were 1.26 nM and 8.2×10^{-5} M^{-1}, respectively.

Figure 23 shows structures of other mercury sensors (83), (84), and (85). Upon adding Hg^{2+} to the coumarin-based sensor (83), a fourfold increment in emission intensity of the band present at 530 nm was observed [162]. The association constant for ML type Hg^{2+} complex was found to be 3.89×10^{5} M^{-1}. Compound (83) was efficiently applied in determining the toxic concentrations of Hg^{2+} in environmental and biological samples. Another weakly fluorescing Schiff base (84) was reported as having $\lambda_{ex}=440$ nm and $\lambda_{em}=530$ nm [163]. It was prepared by simple condensation of coumarin dyes and 5-aminoisophthalic acid methyl ester. The molecule worked effectively in the physiological pH range and was reported to sense nano levels of Hg^{2+} in the living cells. The emission studies done in acetonitrile–water (8:2) medium revealed that the addition of mercury salt to a stock solution of (84) exhibited a broad emission band from 530 to 490 nm with enhancement from 5 to 60 a.u in emission intensity. Mercury is a highly toxic metal that can seriously damage the environment and biological systems. Thus, determining nano levels of mercury in the animal, plant, or human bodies is much needed. Schiff base (85) showed a

Table 5 Distinctive parameters of iron sensors (78)-(81)

Cation sensor	$\lambda_{ex}/\lambda_{em}$ (nm)	M:L ratio	Binding constant (M^{-1})	Detection limit (M)	Mechanism	Reference
(78)	395/506	1:1	1.49×10^{5}	4.6×10^{-6}	CHEQ (turn-off)	[152]
(79)	385/435	1:1	1.52×10^{4}	6.49×10^{-5}	CHEF (turn-on)	[153]
(80)	280/356,372	1:1	7.98×10^{6}	3.75×10^{-8}	LMCT, CHEQ (turn-off)	[154]
(81)	425/526	1:1	1.2×10^{3}	-	CHEQ (turn-off)	[155]

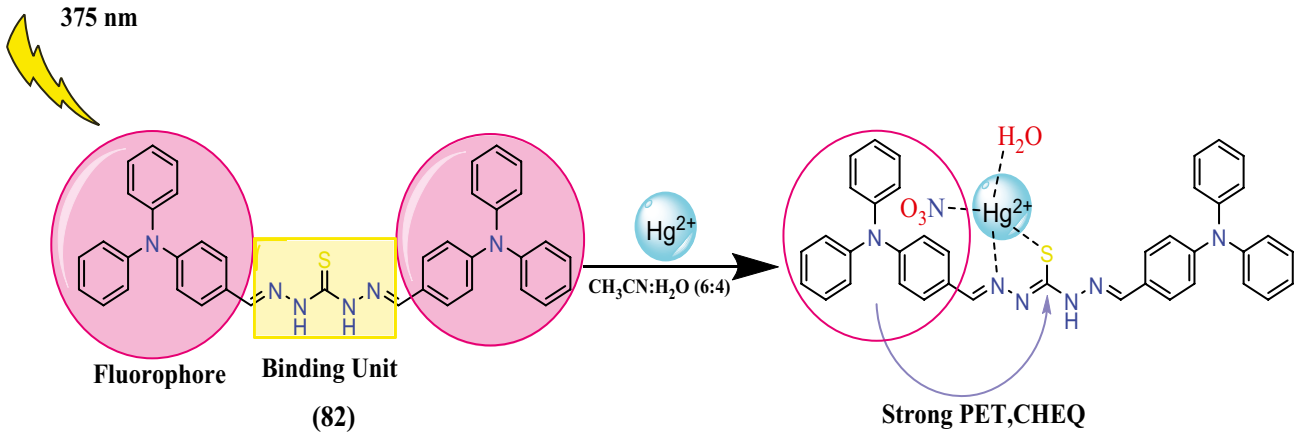

Fig. 22 Proposed binding mechanism of sensor (82) towards Hg^{2+}

turn-on fluorescence response in the existence of mercury ions in an acetonitrile–water (9:1) solvent system, as shown in Fig. 24 [164]. The value of the association constant for the ML_2-type mercury complex is 4.484×10^5 M^{-1}, with the LOD value is 2.268×10^{-8} M for detecting Hg^{2+}.

Fluorescence Sensors for Pb(II)

Divalent lead is one of the harmful metal ions found on the earth, and exposure to very minimal concentrations of it leads to dis-functioning of the digestive and respiratory systems of the human body. As lead is non-biodegradable, it accumulates inside the body and results in severe health disorders such as anemia, loss of memory, muscle paralysis, and neurological dysfunction [165–168].

Detection of the lead ion at the micromolar levels can be achieved with a thiophene-based Schiff base (86) [Fig. 25a] [169]. This molecule showed eightfold enhancement at 490 nm in the presence of Pb^{2+} in a methanol–water (3:1) binary mixture. Further, the yellow solution of the ligand turned red on adding Pb^{2+} into it, making it a colorimetric sensor. The colorimetric and fluorometric detection limits were 6.78 µg/L and 7.38 µg/L, respectively. The fluorescence properties of another Schiff base (87) [Fig. 25b] were explored in an acetonitrile–water (95:5) system [170]. The molecule exhibited weak fluorescence at 508 nm, and in the presence of Pb^{2+}, it showed an 11-fold increase in fluorescence emission, as shown in the spectra [Fig. 26]. The solution studies suggest the formation of a stable M_2L_2-type complex leading to chelation-enhanced fluorescence.

Multi-cation Fluorescence Sensors

The sensors which can detect two or more metal ions simultaneously are called multi-ion sensors. These sensors have various applications in developing test strips for different metal ions, real sample analysis, construction of molecular logic gates, and cell imaging experiments. Some examples of multi-cation sensors (88–112) are discussed in detail.

Schiff bases (88) and (89) were derived from the condensation of 4-(diphenylamino)-2-hydroxybenzaldehyde with cyclohexane-1,2-diamine and ethylene diamine [171]. Both sensors depicted 36-fold enhancement with Zn^{2+} ions ($\lambda_{max} = 488$ nm). Also, the ligands exhibited weak enhancement (fourfold) in the presence of Cd^{2+} ions at $\lambda_{max} = 458$ nm. Interestingly, (88)-Zn^{2+} showed a second turn-on fluorescence phenomenon (190-fold) after adding Cd^{2+} ions and vice-versa. The probes, as mentioned above, detect Mn^{2+} colorimetrically (colorless to orange). The single crystal structure of the zinc complex confirmed the formation of a 1:1 (Zn:L) N_2O_2 coordination complex with square pyramidal geometry. Schiff bases (bis[4-(2-hydroxy-3-methoxybenzyl-ideneamino)phenyl] ether

Fig. 23 Mercury sensors (83), (84) and (85)

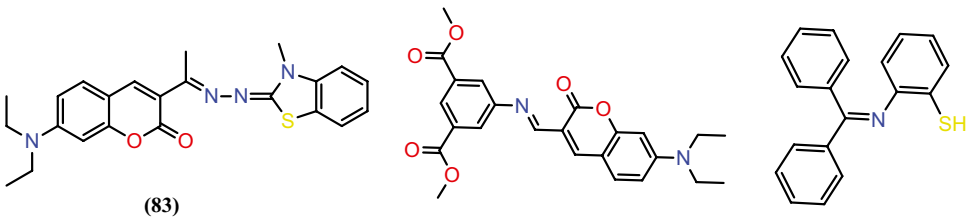

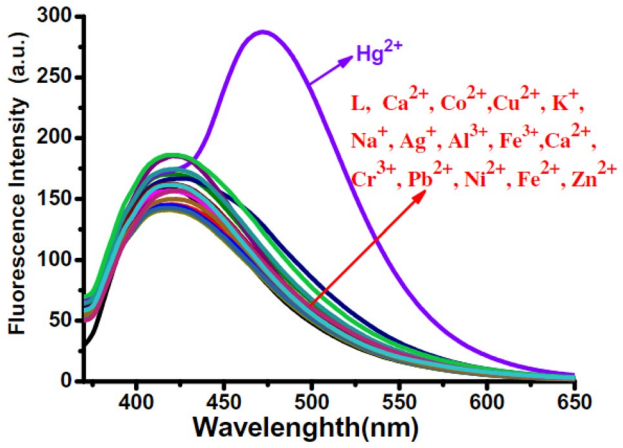

Fig. 24 Fluorescence behavior of probe (85) in presence of metal ions

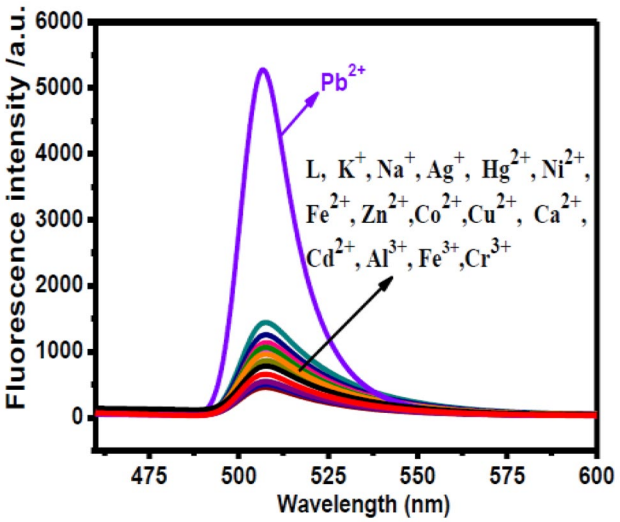

Fig. 26 Fluorescence spectra of (87) in the presence of various metal ions

(90) and(di[(4-phenylimino)4-diethylsalicyl-aldehyde] ether) (91) were used for the simultaneous recognition of biologically important metal ions viz., Al^{3+} and Cr^{3+} in CH_3CN-H_2O (1:1) medium at physiological pH [172]. Probe (90) exhibited a broad emission band at 530 nm, concomitant additions of Al^{3+} and Cr^{3+} caused considerable quenching in ligand's emission, and a new peak was developed at 480 nm (for Al^{3+}) and 508 nm (for Cr^{3+}) displaying hypsochromic shifts. The molecule (91) experienced a very poor emission seen at 490 nm due to the transfer of a proton from phenolic -OH to azomethine 'N' and cis–trans isomerization of C = N. The fluorescence was intensified on complexing with Al^{3+} and Cr^{3+}. Zhu et al. reported another weakly fluorescent Schiff base (92) used to detect Fe^{3+} and Cr^{3+} metal ions simultaneously [173]. It showed a 13-fold enhancement in the emission spectrum with Fe^{3+} and 11-fold with Cr^{3+}, along with a red shift from 495 to 502 nm. All these Schiff bases from (88) to (92), shown in Fig. 27, were weakly fluorescent due to C = N isomerization and the proton transfer mechanism involved; their interaction with the metal ions leads to structural rigidity and enhancement in fluorescence. The other characteristics of these sensors are discussed in Table 6.

2-Hydroxy-N-((9-propyl-9H-carbazol-3-yl)methylene) benzo-hydrazide (95) with a yield of 78.8% was synthesized by condensation of (93) with (94) (41 mg, 0.27 mmol) in anhydrous ethanol at 80 °C [Scheme 8] [174]. This molecule is capable of concurrent sensing of Hg^{2+} and Al^{3+} in a purely aqueous solution. It showed a large quenching at 458 nm with Hg^{2+}, which could be attributed to the CHEQ effect of the heavy metal mercury. Also, (95) marked a rise in the fluorescence intensity and a bathochromic shift with Al^{3+}. This probe also acts as a colorimetric sensor for Al^{3+}, showing a color change from blue to green. LOD for Hg^{2+} and Al^{3+} are 14.7 nM and 47.2 nM, respectively. This probe can be employed for developing test strips, practical sample analysis, molecular logic gate constructions, and cell imaging experiments.

A dual Schiff base sensor 4,4′-Methylenebis[2-[[(2-mercaptophenyl)imino]methyl]phenol (MMIP) (96) [Fig. 28a] was developed successfully by one-pot synthesis [175]. Molecule (96) can detect Ag^{+}, Cu^{2+}, and Hg^{2+} simultaneously over a pH range of 3–10 giving

Fig. 25 **a** Schiff base (86); **b** Structure of M_2L_2 type lead complex of (87)

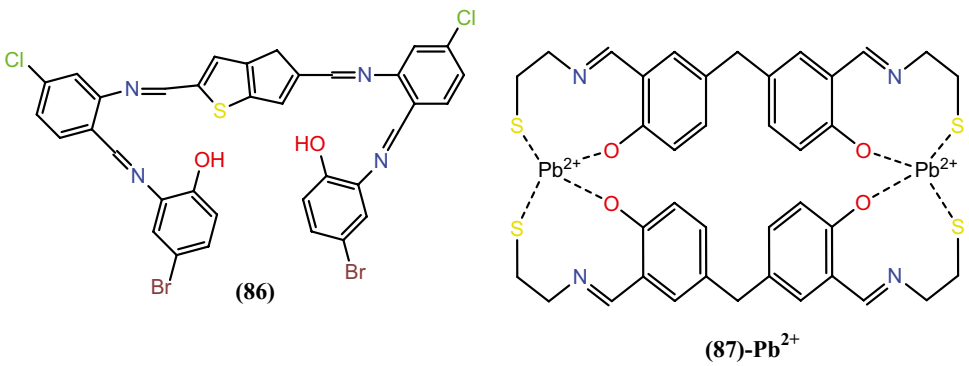

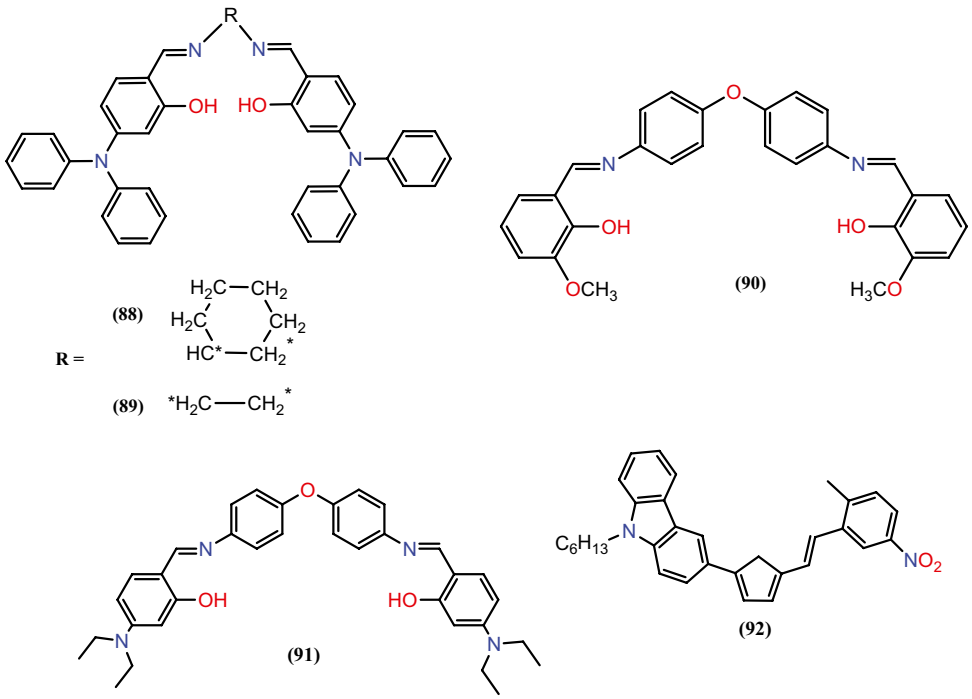

Fig. 27 Structure of multi-ion sensors (88), (89), (90), (91), and (92)

low detection limit values, i.e., 63.7 µM, 64.8 µM, and 52.7 µM, respectively. Investigation of fluorescence properties in DMSO-H_2O (1:1) medium revealed that the molecule having high-intensity emission at $\lambda_{em} = 527$ nm was quenched in the presence of Ag^+, Cu^{2+} and Hg^{2+} as shown in Fig. 28b. Another bifunctional Schiff base (97) [Fig. 28d] consisting of an oligothiophene unit was produced by Zhang [176]. The spectral behavior of this molecule was investigated in the presence and absence of metal ions and found that it recognizes Hg^{2+} and Cu^{2+} in DMSO-H_2O (1:1) solvent mixture, as shown in Fig. 28c. The detection limits were found to be very low, 1.16×10^{-7} M for Hg^{2+} and $7.06 \times 10 - 8$ M for Cu^{2+}. Moreover, regeneration and reversibility studies of the ligand were carried out by adding EDTA solution separately into Cu^{2+} and Hg^{2+} complexes of (97), which regenerates the free ligand.

Crown ethers are a class of macrocyclic compounds having essential applications in forming host–guest complexes. Dong et al. developed a Schiff base chemosensor (98) carrying a phenyl-crown-ether unit, and its interactions with Al^{3+} and Fe^{3+} were highlighted [177]. Upon adding Al^{3+}, the molecule underwent a sharp color change from colorless to orange-yellow, exhibiting a 160-fold fluorescence enhancement, whereas, in the presence of Fe^{3+}, a 130-fold enhancement was registered. In both cases, the CHEF mechanism was involved due to metal ion coordination through four 'N' donors of (98), leading to the formation of a stable, rigid molecular framework [Fig. 29].

The non-fluorescent Schiff base (99) was examined for its photophysical properties with different cations and showed a remarkable increment in fluorescence intensities with zinc and mercury ions [Fig. 30a][178]. This enhancement is primarily due to the restriction of charge transfer happening within the molecule and also for the development of CHEF effect after the formation of respective complexes of ML type [Fig. 30b]. Values of association constants (K_a) calculated from Benesi-Hildebrand plot are

Table 6 Characteristic parameters of Schiff bases (88)-(92)

Cation Sensor	$\lambda_{ex}/\lambda_{em}$ (nm)	M:L ratio	Binding constant (M^1)	Detection limit (M)	Mechanism	Reference
(88)	360/488(Zn^{2+})	1:1	-	-	CHEF, ESIPT, ICT (turn-on)	[171]
	360/458(Cd^{2+})	1:1	-	-		
(90)	350/480(Al^{3+})	1:1	2.35×10^5	1.73×10^{-7}	CHEF, ESIPT, ICT (turn-on)	[172]
	350/508(Cr^{3+})	1:1	1.26×10^5	1.12×10^{-7}		
(91)	430/507(Al^{3+})	1:1	1.46×10^5	4.34×10^{-7}	CHEF, ESIPT, ICT (turn-on)	[172]
	430/486(Cr^{3+})	1:1	3.0×10^5	7.73×10^{-7}		
(92)	380/521(Fe^{3+})	1:2	4.67×10^4	-	CHEF, ESIPT, ICT (turn-on)	[173]
	380/502(Cr^{3+})	1:2	5.97×10^4	-		

Scheme 8 Scheme for the synthesis of Schiff base (95)

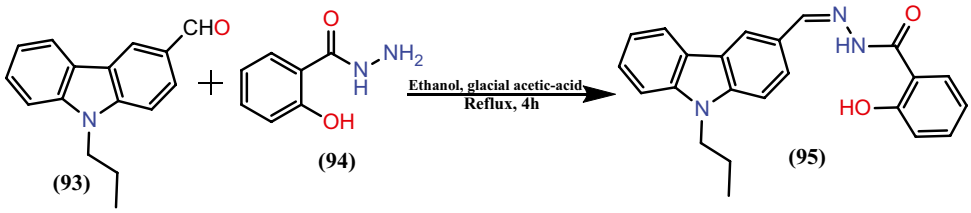

1.52×10^4 M^{-1} for Zn^{2+} and 1.41×10^5 M^{-1} for Hg^{2+}. The molecule can also perform naked-eye detection of Zn^{2+} (colorless to yellow) and Hg^{2+} (colorless to greenish-yellow) ions.

Some other prominent fluorescent sensors (100)-(106) are shown in Fig. 31, along with their binding properties, as listed in Table 7. The sensor (100) was developed explicitly for detecting Al^{3+} and Zn^{2+} [179]. Basically, (100) was a weak fluorescent molecule, but Al^{3+} showed a 196-fold increase in the intensity accompanying the color change from orange to bright yellow. In the case of Zn^{2+}, a 446-fold intensification of the fluorescence intensity was noted, with a new peak appearing at 560 nm. Also, naked-eye detection of Zn^{2+} is possible as color-changed to bright-green. Further application-wise, the authors developed a logic gate circuit by giving emission intensity as an output signal. The reliability of the probe was established in detecting Al^{3+} and Zn^{2+} in real-water samples. The ethanolic solution of Benzimidazole-based Schiff base (101) detects Al^{3+}, $Fe^{3+}$and Cu^{2+} simultaneously in EtOH [180]. It exhibits two emission maxima at 468 and 497 nm. On spectrofluorometric titration with Al^{3+}, an increase in the emission intensity at 497 nm was noticed, which can be substantiated for the ESIPT process. Naked eye detection of Al^{3+} was also possible due to a color change from pale yellow to dark yellow. Further, upon the incremental addition of Cu^{2+} and Fe^{3+} into (101), 15-fold and 11-fold quenching in emission intensity were observed without changing the wavelength maxima. Schiff base (102) was derived through condensation of benzylamine and 2-hydroxybenzaldehyde, which acts as a multi-ion sensor and simultaneously detects Zn^{2+}, Cd^{2+}, and Hg^{2+} with low detection limit value 2.7×10^{-7} M, 7.5×10^{-7} M and 6.0×10^{-7} M respectively [181]. Cytotoxicity analysis of E-(2-(((4-aminophenyl) imino)methyl)-5-(difluorome-thoxy)phenol (103) was done for the liver cancer cells of the HeLa cell line. The results from the cell imaging experiment showed that the percentage of cell viability increased with the increase in the ligand concentration [182]. This molecule was further examined for its fluorescence behavior that showed its recognition for Al^{3+} with an enhancement in emission intensity from 50- 860 a.u in ethanol–water (1:4) as a solvent

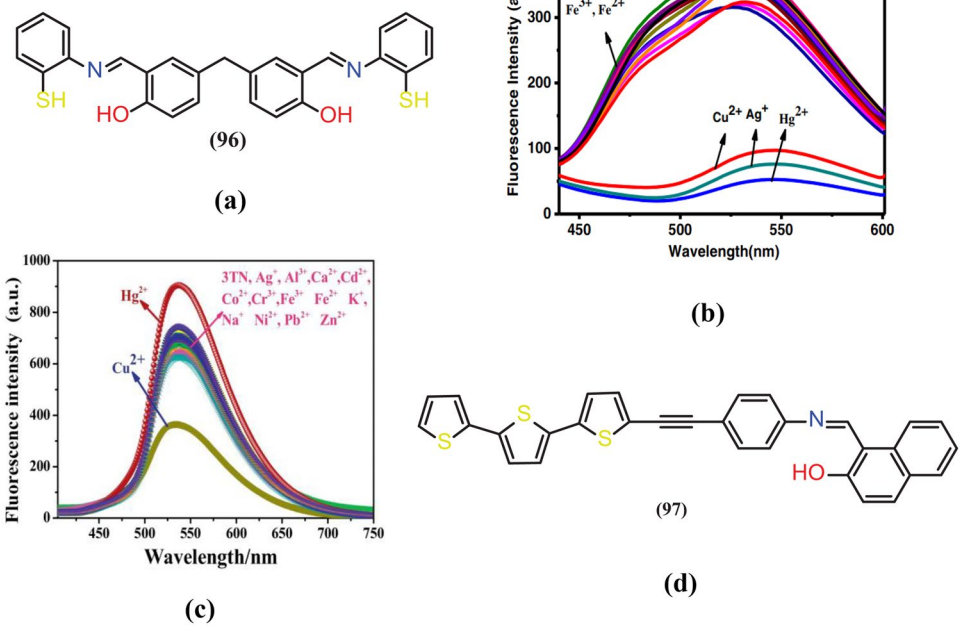

Fig. 28 **a** Structure of sensor (96); **b** Fluorescence spectra of ligand (96) in the presence of metal ions; **c** Emission behavior spectra of ligand (97); **d** Structure of sensor (97)

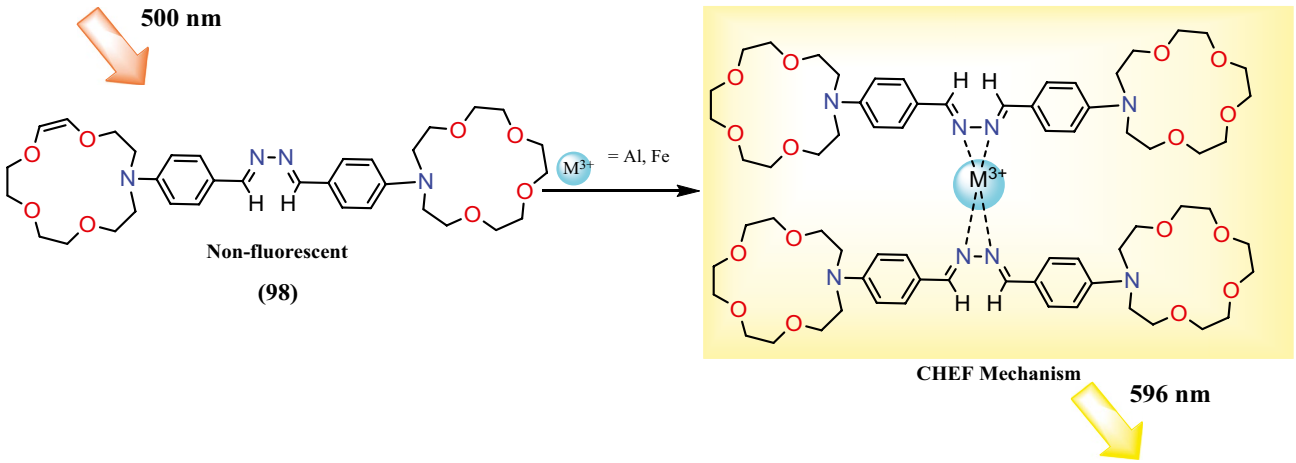

Fig. 29 CHEF mechanism for selective detection of (98) towards Al^{3+} and Fe^{3+}

system. It also showed an increase in the emission intensity in the presence of Fe^{2+} (up to 170 a.u) and Cu^{2+} (395 a.u). These increments in the intensities resulted from the formation of conjugate systems after complexing with the metal ions. Multi-responsive vanilinyl-p-cresol diformyl based imine (104) was developed for simultaneous determination of Zn^{2+} and Cd^{2+}ions [183]. The fluorescence properties of (104) were evaluated in DMSO-water (9:1) binary solvent system with metal ions. A weak intensity emission band was noticed at 482 nm by the ligand only. However, upon adding Zn^{2+} into (104), a 90-fold intensification in the fluorescence intensity was seen. Whereas in the presence of Cd^{2+}, a 120-fold increase was noted. Additionally, the authors developed portable test kits for recognizing Zn^{2+} and Cd^{2+}, where TLC plates were dipped in the solution of this ligand for preparing the test strips. When the dried strips were brought in contact with metal solutions and observed under UV lamps, they showed remarkable color change, i.e., red–orange for Cd^{2+} and red-green for Zn^{2+}. Schiff base (E)-7-(((8-hydroxyquinolin-2-yl)methylene)amino)-4-methyl-2H-chromen-2-one (105) developed by Roy and coworkers selectively detects Fe^{3+} (colorimetrically), Zn^{2+} and Cu^{2+} (fluorometrically) [184]. It displayed a fluorescence band at 438 nm that got manifested by a sixfold increment in the intensity along with a blue shift (438–428 nm) in the presence of Zn^{2+} ions. Contrary, quenching emission intensity 210- 60 a.u was observed with Cu^{2+} ions. A yellow solid, 2-(((9H-fluoren-2-yl)imino)methyl)phenol (106) was obtained with 81% by reaction of 9H-fluoren-2-amine (0.181 g,1 mmol) and 2-hydroxy- benzaldehyde (0.122 g, 1 mmol) in ethanolic solution [185]. The compound was characterized by TLC, melting point, IR, ^{1}H, ^{13}C NMR, and Mass spectroscopy. This probe recognizes both Cr^{3+} and Al^{3+} in an acetonitrile

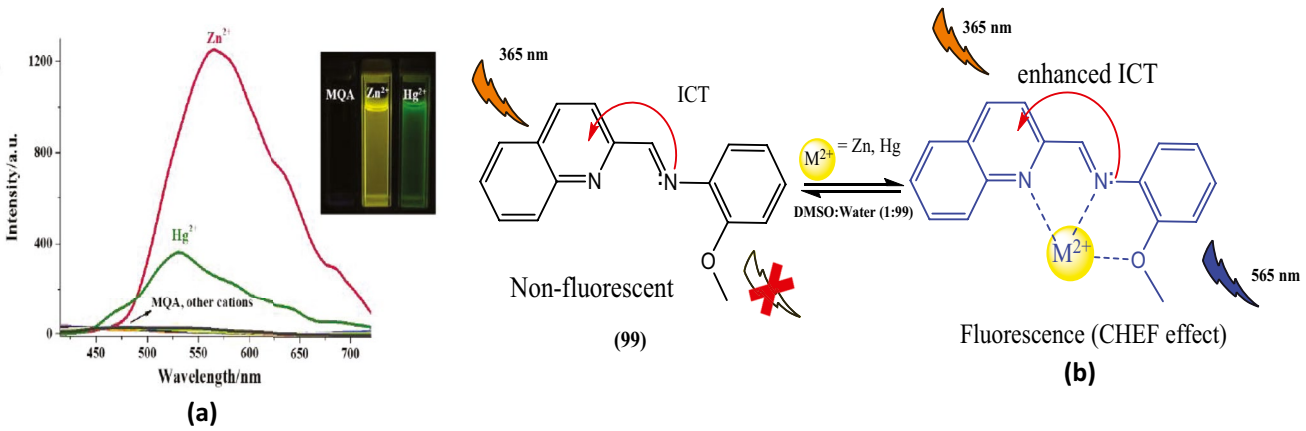

Fig. 30 **a** Emission spectra of (99) in the presence of various metal ions. **b** Plausible binding mechanism of (99) in the presence of Zn^{2+} and Hg^{2+}

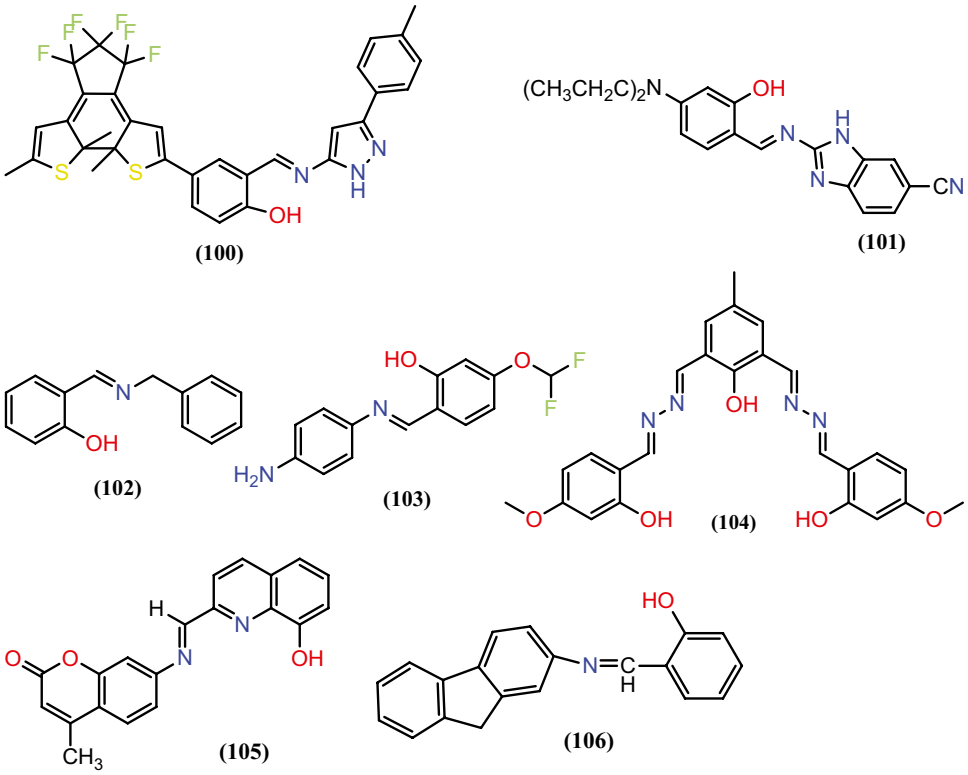

Fig. 31 Structural representation of Schiff bases (100)-(106)

medium by showing an increase in the intensity of the fluorescence band.

2-hydroxy-5-methylisophthalaldehyde and piperazine were reacted to produce Schiff base (107) for successful detection of Zn^{2+} and Cu^{2+} in a water–methanol (9:1) binary-solvent system [186]. The molecule showed a 90-fold increase in emission intensity and a blue shift from 510- 480 nm due to the PET effect's restriction. Also, the

Table 7 Binding properties of Schiff bases (100)-(106)

Cation Sensor	$\lambda_{ex}/\lambda_{em}$ (nm)	M:L ratio	Binding constant (M^{-1})	Detection limit (M)	Mechanism	Reference
(100)	420/58 (Al^{3+})	1:1	1.5×10^{4}	2.7×10^{-7}	CHEF (turn-on)	[179]
	420/560(Zn^{2+})	1:1	6.4×10^{4}	4.0×10^{-8}	CHEF (turn-on)	
(101)	425/497(Cu^{2+})	2:1	1.5×10^{3}	1.3×10^{-7}	Paramagnetic nature (turn-off)	[180]
	424/497(Al^{3+})	1:1	3.5×10^{4}	3.7×10^{-7}		
	425/497(Fe^{3+})	1:1	1.2×10^{9}	-	ESIPT off, (turn-on) CHEQ, turn-off	
(102)	369/452(Zn^{2+})	2:1	-	2.7×10^{-7}	CHEF, (turn-on)	[181]
	369/474(Cd^{2+})	1:1	-	7.5×10^{-7}	CHEF, (turn-on)	
	369/491(Hg^{2+})	2:1	-	6.0×10^{-7}	CHEF, (turn-on)	
(103)	368/478(Al^{3+})	2:1	5.7×10^{4}	13.38 10^{-6}	CHEF (turn-on)	[182]
	439/521(Fe^{2+})	2:1	5.0×10^{4}	-	CHEF (turn-on)	
	473/545(Cu^{2+})	2:1	5.4×10^{4}	-	CHEF (turn-on)	
(104)	482/545(Zn^{2+})	1:1	2.7×10^{4}	2.7×10^{-9}	CHEF (turn-on)	[183]
	482/560(Cd^{2+})	1:1	0.9×10^{4}	6.6×10^{-9}	CHEF (turn-on)	
(105)	335/428(Zn^{2+})	1:1	2.6×10^{4}	-	CHEF, PET off (turn-on)	[184]
	335/438(Cu^{2+})	1:1	8.6×10^{4}	-	Paramagnetic nature (turn-off)	
(106)	333/536(Al^{3+})	2:1	8.3×10^{4}	2.5×10^{-7}	C=N, ESIPT off, (turn-on)	[185]
	333/536(Cr^{3+})	2:1	5.4×10^{4}	3.1×10^{-7}	C=N, ESIPT off, (turn-on)	

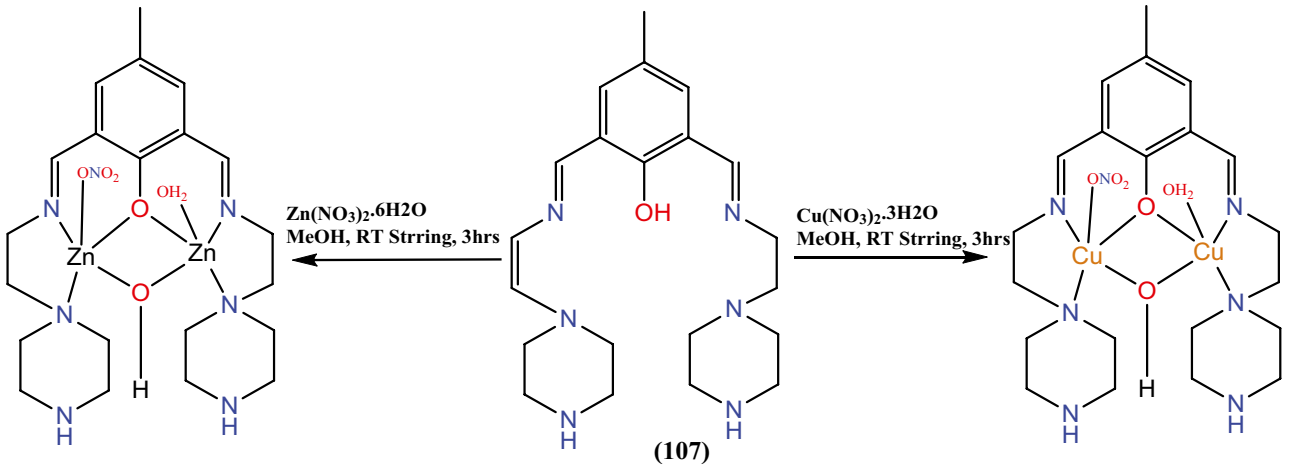

Scheme 9 Route of synthesis for (107)-Zn^{2+} and (107)-Cu^{2+} complexes

C = N isomerization promotes the chelation of Zn^{2+} to (107) through O, N donors forming the M_2L type complex, favoring the CHEF mechanism. However, in the case of Cu^{2+}, 174-fold quenching was seen, possibly due to the paramagnetic nature of Cu^{2+} and the CHEQ mechanism. Seeing their importance in sensor technology, solid complexes of this ligand with Zn^{2+} and Cu^{2+} were synthesized by stirring zinc nitrate hexahydrate (2.0 mmol, 0.5948 g) and copper nitrate trihydrate (2.0 mmol, 0.5912 g) with the Schiff base (107) in ethanol with yield 85% [Scheme 9]. The m/z peaks at 638.00 and 634.14 corresponded to the exact mass of Zn^{2+} and Cu^{2+} complexes, respectively.

Fluorescence imaging studies of a dual coumarin-based sensor (108) were done on the human colon cancer cell [187]. The results depicted that when the cancer cells were treated with this sensor, no fluorescence was observed, but, when the above cells loaded with (108) were exposed to Zn^{2+}, turn-on green fluorescence was seen in the fluorescence microscope. The fluorescence studies revealed that probe (108) initially displayed a weak emission band at 471 nm. After adding Zn^{2+}, this band showed considerable intensity enhancement due to the complex's planarity and rigidity [Fig. 32]. Also, a significant color change from colorless to bright green was observed. The above-said molecule also recognizes Fe^{3+} colorimetrically by a visible difference from colorless to dark brown. The formation constants for Zn^{2+} and Fe^{3+} complexes calculated are 2.847×10^3 M^{-1} and 0.94×10^4 M^{-1}, and the LOD values are 0.6×10^{-8} M and 5.38×10^{-6} M, respectively.

Another Schiff base (109) was a promising tool for simultaneously detecting three metal ions: Hg^{2+}, Cu^{2+}, and Al^{3+}, and behaved as a colorimetric and fluorometric sensor [188]. The notable change in color from yellow to red yellow was seen with Hg^{2+} ions, mainly because of the formation of the Hg^{2+} complex (LOD = 2 μM) involving intra-molecular charge transfer from ligand to metal. Al^{3+} and Cu^{2+} showed enhancement in fluorescence intensities by 216 and 73-fold with LOD values of 2.07 and 1.29 μM, respectively.

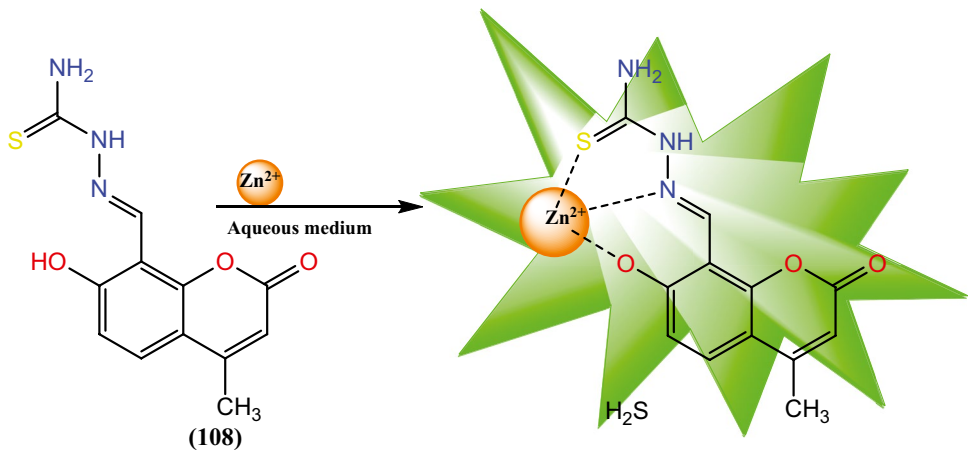

Fig. 32 Fluorescence emission shown by (108) upon formation of Zn^{2+} complex

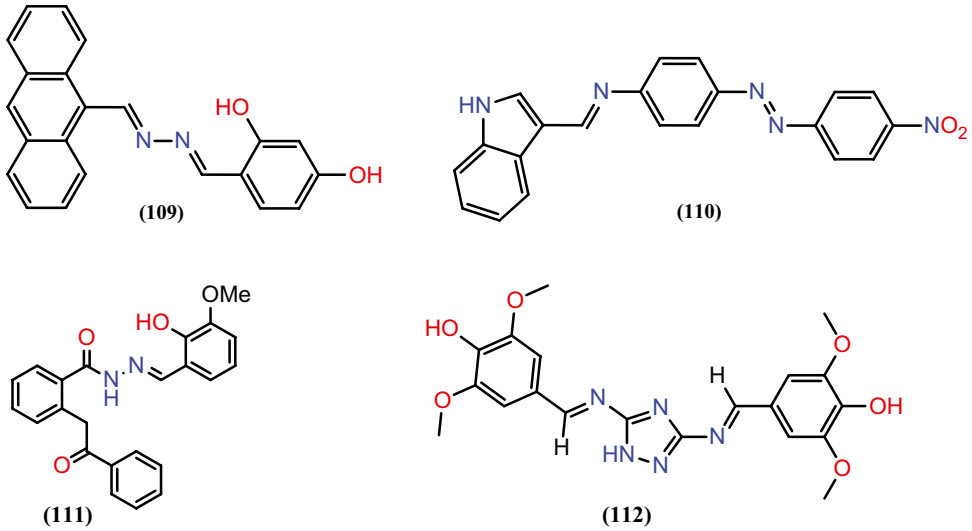

Fig. 33 Structures of probes (109), (110), (111), and (112)

Schiff base4*E*,10*E*-4-(2-(4-nitrophenyl)-*N*-((1H-indol-3-yl) methylene) benzenamine (110) was derived from (4)-4-(phenyldiazenyl)aniline and indole-3-carbaldehyde [189]. This compound showed "Off–On" type emission spectra in the presence of Ni^{2+}, Mg^{2+}, and Fe^{3+} at 487 nm. LOD values calculated for Ni^{2+}, Mg^{2+}, and Fe^{3+} were 6.82×10^{-7} M, 5.27×10^{-7} M, and 5.96×10^{-7} M, respectively. The values of the binding constant computed by the B-H plots method were found to be 3.45×10^{8} M^{-2}, 5.63×10^{4} M^{-2}, and 8.63×10^{3} M^{-2}, respectively. An indole-based Schiff base (110) was checked for its anticancer activity towards the HeLa cell line, results of the experiment showed good in-vitro cytotoxicity behavior of the sensor. Another Schiff base (111) was reported that showed selectivity towards Ni^{2+} and Cu^{2+} amongst the pool of metal cations in the methanol-tris–HCL buffer [190]. This molecule displayed weak emission at 450 nm ($\lambda_{ex}=350$ nm), and an increase in intensity from 250 a.u to 640 a.u was noted with a detection limit of 3.64 µM with Ni^{2+}. On the contrary, adding Cu^{2+} to (111) quenched the emission intensity (250 a.u to 90 a.u), mainly because of the paramagnetic nature of copper metal ions. The stoichiometries of both complexes were 1:1. The probe can detect Ni^{2+} and Cu^{2+} in environmental samples and living cells. Also, this can be used in the construction of INHIBIT-type logic gates. Selective recognition of two important metal ions, such as Pb^{2+} (toxic in nature) and Cu^{2+} (highly essential for plants and animals), was achieved by a single triazole-based compound (112) [191]. The emission studies carried out in CH_3OH–tris-buffer revealed that both Cu^{2+} and Pb^{2+} depicted enhancement in fluorescence intensity about 15-fold and 17-fold, along with LOD values 12×10^{-7} M and 9×10^{-7} M, respectively. The molecule acted as a colorimetric sensor for Cu^{2+} (colorless to yellow), and Pb^{2+} (colorless to light yellow) was noticed through the naked eye. The dual sensor (112) was found useful to check the concentration of Cu^{2+} and Pb^{2+} in water, soil, and biological samples, and also its INHIBIT-logic gate was constructed by the same group. Schiff bases (109)- (112) are shown in Fig. 33.

Applications

Schiff base probes have a wide variety of applications in biological, clinical, and analytical fields [192]. Fluorescence imaging is one of the biomedical applications of such sensors, which allows them to monitor various processes in the cells, tissues, and organs of the body. They are used as a potent tool for live-cell imaging due to their ability to provide non-damaging images of living cells. They are also known for their high selectivity, sensitivity, and fast response time in bacterial detection. For instance, sensors (10), (23), (26), (28), (30), (33), (35), (56), (66), (75), (84), (103), (108), (110) reported in this article were used in cell imaging experiments of various cells including HeLa cells, liver carcinoma cells, zebrafish larvae, human epithelial cells, and human cervical cancer cells, as discussed. The other biomedical applications include drug and biological sample analysis [193–197]. Real sample analysis is another primary application of these sensors, where they are used to directly detect toxic metal ions in real samples such as water, food, soil etc.. Schiff bases (4), (12), (56), (61), (72), (78), (100), (112) reported in this review are practically applied in the real sample analysis. The optical sensing properties of the Schiff base chemosensors are very crucial as they impart applications in the construction of molecular keypads and logic gates due to their molecular switching properties, for example, some already cited sensors: (4), (6), (7), (13), (18), (33), (95), (100), (111),

(112). The metal complexes of Schiff bases offer important industrial applications like catalysis [198]. Other applications include the development of security inks, rewritable papers, and data storage systems [199–201].

Advantages and Disadvantages

Schiff base fluorescence sensors have more advantages over non-Schiff base sensors due to their ease of synthesis with high percentage yield, availability of several binding sites, and variable cavity size in the structural framework that favors complex formation with a wide range of metal ions. The metal chelate effect offers high stability to the Schiff base sensor molecules. Also, a rigid metal–ligand framework influences the emission properties significantly. Most importantly, the preference of the imine group in the Schiff bases enhances the sensor activity by either promoting a blocking ICT, PET, or ESIPT mechanism.

Apart from the merits, these sensors' major drawback is their poor solubility or insolubility in the pure aqueous medium. Most of these molecules are soluble in DMSO/DMF or in combination with other non-polar solvent systems, limiting their applications in biological and environmental fields. However, there still exist several Schiff base sensors that are soluble in an aqueous medium, for example, (4), (5), (16), (35), (38), and (54). A poor detection limit of many sensors that lack high sensitivity and selectivity of the analytes is another concern that needs to be addressed. During the compilation of this presentation, it was felt that the number of Schiff base probes for detecting heavy toxic metal ions such as Hg^{2+}, Pb^{2+}, Cr^{3+}, As^{3+}, Sb^{3+} etc., are less, hence demands more work for new developments for applications in the sensor technology.

Further, the hindrance to precisely detecting ions due to the interference of other coexisting metal ions needs to be sorted out. However, many sensors have high potentiality in sensing due to their promising photophysical properties but are recognized with only limited commercial applications.

Conclusions

The study of fluorescent Schiff base sensors and their binding properties has burgeoned over the past decade. They and their metal complexes are widely used as sensors in medicine, biology, advanced technologies, etc. The simple, time-effective, and low-cost synthesis of Schiff bases and their high coordination ability with various metal ions make them potential candidates for sensing through fluorescence spectroscopy. This review describes several Schiff base probes reported in the last few years, some with the mechanism and their fluorescence sensing ability towards different metal cations. These sensors are crucial because they find places in exploring applications in new developments for environmental and biological metal ions detection. The fluorescence probes used in making transportable realistic test kits for sensing and tracking heavy metal ions in potable water and industrial wastes are highlighted. Also, updates on the successful employment of a number of Schiff base molecules in live cell imaging technique and logic gate construction have been elaborated for young researchers' attention and benefits. Although the binding ability of Schiff bases makes them unique in the detection of various ions, there is still a growing need to focus more on the selectivity and sensitivity aspects of the sensors. A new synthesis of the multifunctional framework with enhanced sensing ability is in demand, along with an exploration of their optical sensing properties for advanced applications. Despite advances in this field, the low selectivity towards most alkali and alkaline earth metal ions is challenging. Despite having excellent sensing efficiency, organic molecule-based sensors often suffer from poor solubility issues and are found unsuitable for bio-application. There should be more focus on the design and synthesis of chemosensors that can work in purely aqueous media. The development of biomimetic and non-toxic sensors is also less explored, limiting the applications of chemosensors in studying living systems. Apart from the challenges mentioned above in designing chemosensors, these sensors can be of great use practically. Compiling the results in this review will help gain insight while designing new Schiff base probes for suitable applications.

Acknowledgements One of the authors(NK) is thankful for the financial assistance from MHRD, India.

Author's Contributions Neha Kumari: Studies, data collection, compilation, and draft preparation; Shalini Singh: Draft preparation, critical revision; MinatiBaral: Conceptualisation, supervision, editing, and correction; B K Kanungo: Editing, formatting, and correction.

Availability of Data and Materials Nil.

Declarations

Ethical Approval This article does not contain any studies involving animals performed by any authors.

Competing Interests The authors declare that they have no competing interests.

References

1. Gokel GW, Leevy WM, Weber ME (2004) Crown ethers: Sensors for ions and molecular scaffolds for materials and biological models. Chem Rev 104:2723–2750. https://doi.org/10.1021/cr020080k

2. Chen X, Pradhan T, Wang F et al (2012) Fluorescent chemosensors based on spiroring-opening of xanthenes and related derivatives. Chem Rev 112:1910–1956. https://doi.org/10.1021/cr200201z
3. Ren Y, Chen X, Li X et al (2010) Quantitative prediction of the thermal motion and intrinsic disorder of protein cofactors in crystalline state: A case study on halide anions. J Theor Biol 266:291–298. https://doi.org/10.1016/j.jtbi.2010.06.038
4. Maurya N, Bhardwaj S, Singh AK (2016) A modest colorimetric chemosensor for investigation of CN- in semi-aqueous environment with high selectivity and sensitivity. Sens Actuators B Chem 229:483–491. https://doi.org/10.1016/j.snb.2016.02.014
5. Michalski R, Kurzyca I (2006) Determination of nitrogen species (nitrate, nitrite and ammonia ions) in environmental samples by ion chromatography. Pol J Environ Stud 15:5–18
6. Upadhyay S, Singh A, Sinha R et al (2019) Colorimetric chemosensors for d-metal ions: A review in the past, present and future prospect. J Mol Struct 1193:89–102. https://doi.org/10.1016/j.molstruc.2019.05.007
7. Erdman JW, Macdonald IA, Zeisel SH (2012) Present Knowledge in Nutrition, 1st edn. Wiley
8. Ross AC, Caballero BH, Cousins RJ, Tucker KL, Ziegler TR (2012) Modern nutrition in health and disease: Eleventh edition. Wolters Kluwer Health Adis (ESP)
9. Ahamed M, Verma S, Kumar A, Siddiqui MKJ (2005) Environmental exposure to lead and its correlation with biochemical indices in children. Sci Total Environ 346:48–55. https://doi.org/10.1016/j.scitotenv.2004.12.019
10. Gaggelli E, Kozlowski H, Valensin D, Valensin G (2006) Copper homeostasis and neurodegenerative disorders (Alzheimer's, Prion, and Parkinson's Diseases and amyotrophic lateral sclerosis). Chem Rev 106:1995–2044. https://doi.org/10.1021/cr040410w
11. Jaishankar M, Tseten T, Anbalagan N et al (2014) Toxicity, mechanism and health effects of some heavy metals. Interdiscip Toxicol 7:60–72. https://doi.org/10.2478/intox-2014-0009
12. Matsui H, Morimoto M, Horimoto K, Nishimura Y (2007) Some characteristics of fluoride-induced cell death in rat thymocytes: Cytotoxicity of sodium fluoride. Toxicol In Vitro 21:1113–1120. https://doi.org/10.1016/j.tiv.2007.04.006
13. Strausak D, Mercer JFB, Dieter HH et al (2001) Copper in disorders with neurological symptoms: Alzheimer's, Menkes, and Wilson diseases. Brain Res Bull 55:175–185. https://doi.org/10.1016/S0361-9230(01)00454-3
14. Botz MM, Mudder TI (2000) Modeling of natural cyanide attenuation in tailings impoundments. Mining Metall Explor 17:228–233. https://doi.org/10.1007/BF03403239
15. Fang G (2001) Spectrophotometric determination of lead in foods with dibromo-p-methyl-bromosulfonazo. Talanta 54:585–589. https://doi.org/10.1016/S00399140(00)00677-9
16. Liu Q, Liu T, Fang Y (2020) Perylene Bisimide derivative-based fluorescent film sensors: From sensory materials to device fabrication. Langmuir 36:2155–2169. https://doi.org/10.1021/acs.langmuir.9b03919
17. Luo X, Han Y, Chen X et al (2020) Carbon dots derived fluorescent nanosensors as versatile tools for food quality and safety assessment: A review. Trends Food Sci Technol 95:149–161. https://doi.org/10.1016/j.tifs.2019.11.017
18. Shamsipur M, Barati A, Nematifar Z (2019) Fluorescent pH nanosensors: Design strategies and applications. J Photochem Photobiol C 39:76–141. https://doi.org/10.1016/j.jphotochemrev.2019.03.001
19. Velusamy S, Roy A, Sundaram S, Kumar Mallick T (2021) A review on heavy metal ions and containing dyes removal through graphene oxide-based adsorption strategies for textile wastewater treatment. Chem Rec 21:1570–1610. https://doi.org/10.1002/tcr.202000153
20. Becker JS, Matusch A, Depboylu C et al (2007) Quantitative imaging of selenium, copper, and zinc in thin sections of biological tissues (slugs−genus arion) measured by laser ablation inductively coupled plasma mass spectrometry. Anal Chem 79:6074–6080. https://doi.org/10.1021/ac0700528
21. Liu Y, Liang P, Guo L (2005) Nanometer titanium dioxide immobilized on silica gel as sorbent for preconcentration of metal ions prior to their determination by inductively coupled plasma atomic emission spectrometry. Talanta 68:25–30. https://doi.org/10.1016/j.talanta.2005.04.035
22. Wang X, Sun J, Tong J et al (2018) Paper-based sensor chip for heavy metal ion detection by SWSV. Micromachines 9:150. https://doi.org/10.3390/mi9040150
23. Barba-Bon A, Costero AM, Gil S et al (2012) A new selective fluorogenic probe for trivalent cations. Chem Commun 48:3000. https://doi.org/10.1039/c2cc17184h
24. Kaur B, Kaur N, Kumar S (2018) Colorimetric metal ion sensors – A comprehensive review of the years 2011–2016. Coord Chem Rev 358:13–69. https://doi.org/10.1016/j.ccr.2017.12.002
25. Sarkar M (2020) A review on 2,6-Diformyl-4-methylphenol derived schiff bases as fluorescent sensors. Asian J Chem 32:1837–1848. https://doi.org/10.14233/ajchem.2020.22644
26. Wright AT, Anslyn EV (2006) Differential receptor arrays and assays for solution-based molecular recognition. Chem Soc Rev 35:14–28. https://doi.org/10.1039/B505518K
27. Amendola V, Fabbrizzi L (2009) Anion receptors that contain metals as structural units. ChemCommun 513–531. https://doi.org/10.1039/B808264M
28. Prodi L (2005) Luminescent chemosensors: from molecules to nanoparticles. New J Chem 29:20. https://doi.org/10.1039/b411758a
29. Yoon J, Kim SK, Singh NJ, Kim KS (2006) Imidazolium receptors for the recognition of anions. Chem Soc Rev 35:355. https://doi.org/10.1039/b513733k
30. Czarnik AW (1994) Fluorescent chemosensors for ion and molecule recognition. Instrum Sci Technol 22:405–406. https://doi.org/10.1080/10739149408001201
31. Kumar A, Virender MB et al (2022) Development of 2-hydroxy-naphthaldehyde functionalized Schiff base chemosensor for spectroscopic and colorimetric detection of Cu^{2+} and Pd^{2+} ions. Microchem J 180:107561. https://doi.org/10.1016/j.microc.2022.107561
32. Yin P, Ma W, Liu J et al (2022) Dual functional chemosensor for nano-level detection of Al^{3+} and Cu^{2+}: Application to real samples analysis, colorimetric test strips and molecular logic gates. Microchem J 180:107557. https://doi.org/10.1016/j.microc.2022.107557
33. Yu W, Wang L, Wang L et al (2021) Quinoline based colorimetric and "turn-off" fluorescent chemosensor for phosgene sensing in solution and vapor phase. Microchem J 168:106334. https://doi.org/10.1016/j.microc.2021.106334
34. Udhayakumari D, Naha S, Velmathi S (2017) Colorimetric and fluorescent chemosensors for Cu^{2+}. A comprehensive review from the years 2013–15. Anal Methods 9:552–578. https://doi.org/10.1039/C6AY02416E
35. Abu-Dief AM, Mohamed IMA (2015) A review on versatile applications of transition metal complexes incorporating Schiff bases. Beni-Suef Univ J Basic Appl Sci 4:119–133. https://doi.org/10.1016/j.bjbas.2015.05.004
36. Qin W, Long S, Panunzio M, Biondi S (2013) Schiff bases: a short survey on an evergreen chemistry tool. Molecules 18:12264–12289. https://doi.org/10.3390/molecules181012264
37. Antony R, Arun T, Manickam STD (2019) A review on applications of chitosan-based schiff bases. Int J Biol Macromol 129:615–633. https://doi.org/10.1016/j.ijbiomac.2019.02.047
38. Kajal A, Bala S, Kamboj S et al (2013) Schiff bases: A versatile pharmacophore. J Catal 2013:1–14. https://doi.org/10.1155/2013/893512
39. Muzammil K, Trivedi P, Ketani DB (2015) Synthesis and characterization of schiff base m-nitro aniline and their complexes. Res J Chem 5:52–55

40. Kolapwar BG (2017) Study of Schiff base compounds and its derivatives. Anveshana's Int J Rese Pharm Life Sci 2:15–18
41. Salvat A, Fortunato, et al (2001) Screening of some plants from Northern Argentina for their antimicrobial activity. Lett ApplMicrobiol 32:293–297. https://doi.org/10.1046/j.1472-765X.2001.00923.x
42. Fareed G, Rizwani GH, Ahmed M et al (2017) Schiff bases derived from 1-aminoanthraquinone: A new class of analgesic compounds. Pak J Sciind Res Ser A Physsci 60:122–127. https://doi.org/10.52763/PJSIR.PHYS.SCI.60.3.2017.122.127
43. Hanif M, Hassan M, Rafiq M et al (2018) Microwave-assisted synthesis, in vivo anti-inflammatory and in vitro anti-oxidant activities, and molecular docking study of new substituted schiff base derivatives. Pharm Chem J 52:424–437. https://doi.org/10.1007/s11094-018-1835-0
44. Kakanejadifard A, Khojasteh V, Zabardasti A, Azarbani F (2018) New azo-schiff base ligand capped silver and cadmium sulfide nanoparticles preparation, characterization, antibacterial and antifungal activities. Org Chem Res. https://doi.org/10.22036/org.chem.2018.133383.1149
45. Malik A, Goyat G, Verma KK, Garg S (2018) Synthesis, spectral and antimicrobial studies of some o-vanillin-2-aminopyridine schiff base complexes of organyltellurium (IV). Chem Sci Trans. https://doi.org/10.7598/cst2018.1480
46. Kalaiarasi G, Dharani S, Puschmann H, Prabhakaran R (2018) Synthesis, structural characterization, DNA/protein binding and antioxidant activities of binuclear Ni(II) complexes containing ONS chelating ligands bridged by 1,3-bis(diphenylphosphino) propane. Inorg Chem Commun 97:34–38. https://doi.org/10.1016/j.inoche.2018.09.004
47. Al-Shemary RK (2017) Design, synthesis and biological evaluation of schiff bases and their Co(II), Cu(II), Ni(II) chelates from derivative containing indole moiety bearing-triazole. ECB 6:433. https://doi.org/10.17628/ecb.2017.6.433-439
48. Luo H, Xia Y, Sun B et al (2017) Synthesis and evaluation of in vitro antibacterial and antitumor activities of novel N, N-disubstituted schiff bases. Biochem Res Int 2017:1–10. https://doi.org/10.1155/2017/6257240
49. More G, Bootwala SZ, Mascarenhas J, Aruna K (2018) Antimicrobial and anti-tubercular activity evaluation of newly synthesized zinc complexes of aminothiophene schiff bases. Int J Pharm Sci Res 9:3029–3035. https://doi.org/10.13040/IJPSR.0975-8232.9(7)
50. Mahmood Yousif Al-Labban H, Mohammed Sadiq H, AbduljabbarJaloobAljanaby A (2019) Synthesis, Characterization and study biological activity of some Schiff bases derivatives from 4-amino antipyrine as a starting material. J Phys Conf Ser 1294:052007. https://doi.org/10.1088/1742-6596/1294/5/052007
51. Peng H, Liu Y, Huang J et al (2021) A simple fluorescent probe for selective detection of Al^{3+} based on furan Schiff base and its crystal structure. J Mol Struct 1229:129866. https://doi.org/10.1016/j.molstruc.2020.129866
52. Shin H, Jannah F, Yoo EJ, Kim J-M (2022) A colorimetric and fluorescence "turn-on" sensor for Fe(III) ion based on imidazole-functionalized polydiacetylene. Sens Actuators B Chem 350:130885. https://doi.org/10.1016/j.snb.2021.130885
53. Tümay SO, Yeşilot S (2021) Highly selective "turn-on" fluorescence determination of mercury ion in food and environmental samples through novel anthracene and pyrene appended Schiff bases. J Photochem Photobiol A 407:113093. https://doi.org/10.1016/j.jphotochem.2020.113093
54. Mohanasundaram D, Bhaskar R, Sankarganesh M et al (2022) A simple pyridine based fluorescent chemosensor for selective detection of copper ion. Spectrochim Acta Part A Mol Biomol Spectrosc 265:120395. https://doi.org/10.1016/j.saa.2021.120395
55. Chauhan A, Langyan R (2022) Photosensitization in highly luminescent nonmacrocyclic Samarium(III) complexes for application in light-emitting systems. J Photochem Photobiol A 424:113627. https://doi.org/10.1016/j.jphotochem.2021.113627
56. Ding W, Wu Y, Zhang S et al (2021) A dual-channel 'turn-on' fluorescent chemosensor for high selectivity and sensitivity detection of CN^- based on a coumarin-Schiff base derivative in an aqueous system. Luminescence 36:1306–1316. https://doi.org/10.1002/bio.4058
57. Singh H, Bamrah A, Bhardwaj SK et al (2021) Recent advances in the application of noble metal nanoparticles in colorimetric sensors for lead ions. Environ Sci Nano 8:863–889. https://doi.org/10.1039/D0EN00963F
58. Sun X, Ding Y, Niu B, Chen Q (2021) Evaluation of a composite nanomaterial consist of gold nanoparticles and graphene-carbon nitride as capillary electrochromatography stationary phase for enantioseparation. Microchem J 169:106613. https://doi.org/10.1016/j.microc.2021.106613
59. Udhayakumari D, Inbaraj V (2020) A review on schiff base fluorescent chemosensors for cell imaging applications. J Fluoresc 30:1203–1223. https://doi.org/10.1007/s10895-020-02570-7
60. Junaid HM, Batool M, Harun FW et al (2022) Naked eye chemosensing of anions by schiff bases. Crit Rev Anal Chem 52:463–480. https://doi.org/10.1080/10408347.2020.1806703
61. Shah SS, Shah D, Khan I, Ahmad S, Ali U, Rahman AU (2020) Synthesis and antioxidant activities of schiff bases and their complexes: An updated review. Biointerface Res Appl Chem 10:6936–6963. https://doi.org/10.33263/BRIAC106.69366963
62. Al Zoubi W, Ko YG (2017) Schiff base complexes and their versatile applications as catalysts in oxidation of organic compounds: part I: Schiff bases and their versatile applications. Appl Organometal Chem 31:3574. https://doi.org/10.1002/aoc.3574
63. Gupta P, Dwivedi D, Chourey VR (2021) Review article on metal complexes derived from 2'-hydroxyacetophenone based Schiff Base. Orient J Chem 37:25–32. https://doi.org/10.13005/ojc/370102
64. Uddin MN, Ahmed SS, Alam SMR (2020) REVIEW: Biomedical applications of Schiff base metal complexes. J Coord Chem 73:3109–3149. https://doi.org/10.1080/00958972.2020.1854745
65. Shetty P (2020) Schiff bases: An overview of their corrosion inhibition activity in acid media against mild steel. Chem Eng Commun 207:985–1029. https://doi.org/10.1080/00986445.2019.1630387
66. Berhanu AL, Gaurav MI et al (2019) A review of the applications of Schiff bases as optical chemical sensors. TrAC, Trends Anal Chem 116:74–91. https://doi.org/10.1016/j.trac.2019.04.025
67. Naskar B, Modak R, Sikdar Y et al (2017) Fluorescent sensing of $Al^{3+}$by benzophenone-based Schiff base chemosensor and live cell imaging applications: Impact of keto-enol tautomerism. Sens Actuators B Chem 239:1194–1204. https://doi.org/10.1016/j.snb.2016.08.148
68. Sen B, Sheet SK, Thounaojam R et al (2017) A coumarin based Schiff base probe for selective fluorescence detection of Al^{3+} and its application in live cell imaging. Spectrochim Acta Part A Mol Biomol Spectrosc 173:537–543. https://doi.org/10.1016/j.saa.2016.10.005
69. Sharma S, Hundal MS, Walia A et al (2014) Nanomolar fluorogenic detection of Al(III) by a series of Schiff bases in an aqueous system and their application in cell imaging. Org Biomol-Chem 12:4445. https://doi.org/10.1039/c4ob00329b
70. Fan L, Qin J, Li T et al (2014) A chromone Schiff-base as Al(III) selective fluorescent and colorimetric chemosensor. J Lumin 155:84–88. https://doi.org/10.1016/j.jlumin.2014.06.023
71. Kashyap KS, Kumar A, Hira SK, Dey S (2019) Recognition of Al^{3+} through the off-on mechanism as a proficient driving force for the hydrolysis of BODIPY conjugated Schiff base and its application in bio-imaging. Inorganica Chim Acta 498:119157. https://doi.org/10.1016/j.ica.2019.119157

72. Xu Y, Li L, Bai L et al (2020) Water-soluble fluorescent chemosensor based on Schiff base derivative terminated PEG for highly efficient detection of Al^{3+} in pure aqueous media. Tetrahedron Lett 61:152335. https://doi.org/10.1016/j.tetlet.2020.152335
73. Xu Y, Kong L, Bai L et al (2021) A new water-soluble polymer fluorescent chemosensor with thiophene Schiff base site for selectively sensing Al^{3+} ions. Tetrahedron 79:131888. https://doi.org/10.1016/j.tet.2020.131888
74. Selvan GT, Kumaresan M, Sivaraj R et al (2016) Isomeric 4-aminoantipyrine derivatives as fluorescent chemosensors of Al^{3+} ions and their molecular logic behaviour. Sens Actuators B Chem 229:181–189. https://doi.org/10.1016/j.snb.2016.01.097
75. Xu H, Chen W, Ju L, Lu H (2021) A purine based fluorescent chemosensor for the selective and sole detection of Al^{3+} and its practical applications in test strips and bio-imaging. Spectrochim Acta Part A Mol Biomol Spectrosc 247:119074. https://doi.org/10.1016/j.saa.2020.119074
76. Xu J, Li H, Li L et al (2020) A highly selective fluorescent chemosensor for Al^{3+} Based on 2,2':6',2"-terpyridine with a salicylal schiff base. J Braz Chem Soc. https://doi.org/10.21577/0103-5053.20200063
77. Chen Y (2020) Microwave-assisted synthesis of a novel steroid-derived Schiff base chemosensor for detection of Al^{3+} in aqueous media. J Chem Res 44:750–755. https://doi.org/10.1177/1747519820914827
78. Banerjee S, Brandão P, Saha A (2016) A robust fluorescent chemosensor for aluminum ion detection based on a Schiff base ligand with an azo arm and application in a molecular logic gate. RSC Adv 6:101924–101936. https://doi.org/10.1039/C6RA21217D
79. Gao C, Zang P, Liu W, Tang Y (2016) A highly selective and sensitive fluorescent chemosensor for aluminum ions based on schiff base. J Fluoresc 26:2015–2021. https://doi.org/10.1007/s10895-016-1895-z
80. Hossain SM, Singh K, Lakma A et al (2017) A schiff base ligand of coumarin derivative as an ICT-Based fluorescence chemosensor for Al^{3+}. Sens Actuators B Chem 239:1109–1117. https://doi.org/10.1016/j.snb.2016.08.093
81. Hwang IH, Choi YW, Kim KB et al (2016) A highly selective and sensitive fluorescent turn-on Al^{3+} chemosensor in aqueous media and living cells: experimental and theoretical studies. New J Chem 40:171–178. https://doi.org/10.1039/C5NJ02334C
82. Alyaninezhad Z, Bekhradnia A, Feizi N et al (2019) A novel aluminum-sensitive fluorescent chemosensor based on 4-aminoantipyrine: An experimental and theoretical study. Spectrochim Acta Part A Mol Biomol Spectrosc 212:32–41. https://doi.org/10.1016/j.saa.2018.12.035
83. Manna AK, Chowdhury S, Patra GK (2020) Combined experimental and theoretical studies on a phenyl thiadiazole-based novel turn-on fluorescent colorimetric Schiff base chemosensor for the selective and sensitive detection of Al^{3+}. New J Chem 44:10819–10832. https://doi.org/10.1039/D0NJ01954B
84. Kim SY, Lee SY, Kang JH et al (2018) Colorimetric detection of $Fe^{3+/2+}$ and fluorescent detection of Al^{3+} in aqueous media: applications and DFT calculations. J Coord Chem 71:2401–2414. https://doi.org/10.1080/00958972.2018.1478086
85. Kurbah SD, Kumar A, Shangpung S et al (2017) Synthesis, characterization, and fluorescence chemosensor properties of a *cis* -dioxomolybdenum (VI) complex containing multidentate hydrazone ligands. Z Anorg Allg Chem 643:794–801. https://doi.org/10.1002/zaac.201700100
86. Li H, Wang J, Zhang S et al (2018) A novel off-on fluorescent chemosensor for Al^{3+} derived from a 4,5-diazafluorene Schiff base derivative. RSC Adv 8:31889–31894. https://doi.org/10.1039/C8RA05280H
87. Liu T, Wan X, Dong Y et al (2017) Facile synthesis of a water-soluble fluorescence sensor for Al^{3+} in aqueous solution and on paper substrate. Spectrochim Acta Part A Mol Biomol Spectrosc 173:625–629. https://doi.org/10.1016/j.saa.2016.10.004
88. Naskar B, Modak R, Sikdar Y et al (2017) Fluorescent sensing of Al^{3+} by benzophenone-based Schiff base chemosensor and live cell imaging applications: Impact of keto-enol tautomerism. Sens Actuators B Chem 239:1194–1204. https://doi.org/10.1016/j.snb.2016.08.148
89. Selvan GT, Kumaresan M, Sivaraj R et al (2016) Isomeric 4-aminoantipyrine derivatives as fluorescent chemosensors of Al^{3+} ions and their molecular logic behavior. Sens Actuators B Chem 229:181–189. https://doi.org/10.1016/j.snb.2016.01.097
90. Tian H, Qiao X, Zhang Z-L et al (2019) A high performance 2-hydroxynaphthalene schiff base fluorescent chemosensor for Al^{3+} and its applications in imaging of living cells and zebrafish in vivo. Spectrochim Acta Part A Mol Biomol Spectrosc 207:31–38. https://doi.org/10.1016/j.saa.2018.08.063
91. Andreini C, Banci L, Bertini I, Rosato A (2006) Zinc through the three domains of life. J Proteome Res 5:3173–3178. https://doi.org/10.1021/pr0603699
92. Bhowmick R, Alam R, Mistri T et al (2016) A thiosemicarbazone based chemo and fluorogenic sensor for Zn $^{2+}$ with CHEF and ESIPT behavior: computational studies and cell imaging application. RSC Adv 6:11388–11399. https://doi.org/10.1039/C5RA25653D
93. Mantyh PW, Ghilardi JR, Rogers S et al (1993) Aluminum, iron, and zinc ions promote aggregation of physiological concentrations of β-amyloid peptide. J Neurochem 61:1171–1174. https://doi.org/10.1111/j.1471-4159.1993.tb03639.x
94. Yanagisawa H, Miyakoshi Y, Kobayashi K et al (2009) Long-term intake of a high zinc diet causes iron deficiency anemia accompanied by reticulocytosis and extra-medullary erythropoiesis. Toxicol Lett 191:15–19. https://doi.org/10.1016/j.toxlet.2009.07.024
95. Ahmed N, Zareen W, Zhang D et al (2020) A DCM-based NIR sensor for selective and sensitive detection of Zn^{2+} in living cells. Spectrochim Acta Part A Mol Biomol Spectrosc 243:118758. https://doi.org/10.1016/j.saa.2020.118758
96. Choi YW, You GR, Lee JJ, Kim C (2016) Turn-on fluorescent chemosensor for selective detection of Zn^{2+} in an aqueous solution: Experimental and theoretical studies. Inorg Chem Commun 63:35–38. https://doi.org/10.1016/j.inoche.2015.11.012
97. Gomathi A, Vasanthi M, Viswanthamurthi P et al (2018) A simple perceptive diphenyl-imidazole-based dipodal schiff-base chemosensor for Zn^{2+} and PPi ions and its live-cell imaging applications. ChemistrySelect 3:11809–11815. https://doi.org/10.1002/slct.201802233
98. Berrones-Reyes JC, Muñoz-Flores BM, Cantón-Diáz AM et al (2019) Quantum chemical elucidation of the turn-on luminescence mechanism in two new Schiff bases as selective chemosensors of Zn^{2+} : synthesis, theory and bioimaging applications. RSC Adv 9:30778–30789. https://doi.org/10.1039/C9RA05010H
99. Feng E, Tu Y, Fan C et al (2017) A highly selective and sensitive fluorescent chemosensor for Zn^{2+} based on a diarylethene derivative. RSC Adv 7:50188–50194. https://doi.org/10.1039/C7RA09966E
100. Sarkar D, Pramanik A, Jana S et al (2015) Quinoline based reversible fluorescent 'turn-on' chemosensor for the selective detection of Zn^{2+}: Application in living cell imaging and as INHIBIT logic gate. Sens Actuators B Chem 209:138–146. https://doi.org/10.1016/j.snb.2014.11.097
101. Rout K, Manna AK, Sahu M, Patra GK (2019) A guanidine based bis schiff base chemosensor for colorimetric detection of Hg(II) and fluorescent detection of Zn(II) ions. Inorganica Chim Acta 486:733–741. https://doi.org/10.1016/j.ica.2018.11.021
102. Kim MS, Jo TG, Yang M et al (2019) A fluorescent and colorimetric Schiff base chemosensor for the detection of Zn^{2+} and

Cu^{2+}: Application in live cell imaging and colorimetric test kit. Spectrochim Acta Part A Mol Biomol Spectrosc 211:34–43. https://doi.org/10.1016/j.saa.2018.11.058
103. Kumar M, Kumar A, Singh MK et al (2017) A novel benzidine based Schiff base "turn-on" fluorescent chemosensor for selective recognition of Zn^{2+}. Sens Actuators B Chem 241:1218–1223. https://doi.org/10.1016/j.snb.2016.10.008
104. Li H, Zhang S, Gong C et al (2016) A turn-on and reversible fluorescence sensor for zinc ion based on 4,5-diazafluorene schiff base. J Fluoresc 26:1555–1561. https://doi.org/10.1007/s10895-016-1877-1
105. Shamel A, Salemnoush T (2016) Synthesis and fluorescence study of the grafted salicylidene schiff base onto SBA-15 mesoporous silica for detecting Zn^{2+} traces in aqueous medium. Russ J Appl Chem 89:500–504. https://doi.org/10.1134/S10704272160030228
106. Wang W, Li R, Song T et al (2016) Study on the fluorescent chemosensors based on a series of bis-Schiff bases for the detection of zinc(II). Spectrochim Acta Part A Mol Biomol Spectrosc 164:133–138. https://doi.org/10.1016/j.saa.2016.04.016
107. Yan J, Fan L, Qin J et al (2016) A novel and resumable schiff-base fluorescent chemosensor for Zn(II). Tetrahedron Lett 57:2910–2914. https://doi.org/10.1016/j.tetlet.2016.05.079
108. Wang X, Ding G, Duan Y et al (2020) Novel 'naked-eye' bis-schiff base fluorescent chemosensors for sensitive detection of Zn^{2+} and bio-imaging in living cells. Tetrahedron 76:131108. https://doi.org/10.1016/j.tet.2020.131108
109. Lee SY, Bok KH, Kim JA et al (2016) Simultaneous detection of Cu^{2+} and Cr^{3+} by a simple Schiff-base colorimetric chemosensor bearing NBD (7-nitrobenzo-2-oxa-1,3-diazolyl) and julolidine moieties. Tetrahedron 72:5563–5570. https://doi.org/10.1016/j.tet.2016.07.051
110. Murugesan K, Jeyasingh V, Lakshminarayanan S et al (2019) Simple and highly electron deficient schiff-base host for anions: First turn-on colorimetric bifluoride sensor. Spectrochim Acta Part A Mol Biomol Spectrosc 209:165–169. https://doi.org/10.1016/j.saa.2018.10.043
111. Udhayakumari D, Velmathi S (2015) Azo linked polycyclic aromatic hydrocarbons-based dual chemosensor for Cu^{2+} and Hg^{2+} ions. Ind Eng Chem Res 54:3541–3547. https://doi.org/10.1021/acs.iecr.5b00775
112. Basaki M, Saeb M, Nazifi S, Shamsaei HA (2012) Zinc, copper, iron, and chromium concentrations in young patients with type 2 diabetes mellitus. Biol Trace Elem Res 148:161–164. https://doi.org/10.1007/s12011-012-9360-6
113. De Romaña DL, Olivares M, Uauy R, Araya M (2011) Risks and benefits of copper in light of new insights of copper homeostasis. J Trace Elem Med Biol 25:3–13. https://doi.org/10.1016/j.jtemb.2010.11.004
114. Zhang Y, Cao X, Zhen L, Wang X (2021) A mesoporous silica-based fluorescent chemosensor bearing bis-Schiff base for the sensitive detection of Cu^{2+} ions. J Solid-State Chem 297:122093. https://doi.org/10.1016/j.jssc.2021.122093
115. Moradinia E, Mansournia M, Notash B (2019) A turn-off fluorescent chemosensor for Cu(II) based on sensitive Schiff base derived from 4-tert-Butyl-2,6-diformylphenol and p-toluic hydrazide. J Photochem Photobiol A 382:111963. https://doi.org/10.1016/j.jphotochem.2019.111963
116. Liang S, Tong Q, Qin X et al (2020) A hydrophilic naphthalimide-based fluorescence chemosensor forCu^{2+} ion: Sensing properties, cell imaging and molecular logic behavior. Spectrochim Acta Part A Mol Biomol Spectrosc 230:118029. https://doi.org/10.1016/j.saa.2020.118029
117. Rathod RV, Bera S, Singh M, Mondal D (2016) A colorimetric and fluorometric investigation of Cu(II) ion in aqueous medium with a fluorescein-based chemosensor. RSC Adv 6:34608–34615. https://doi.org/10.1039/C6RA03021A
118. Sadia M, Naz R, Khan J, Khan R (2018) Synthesis and evaluation of a schiff-based fluorescent chemosensors for the selective and sensitive detection of Cu^{2+} in aqueous media with fluorescence off-on responses. J Fluoresc 28:1281–1294. https://doi.org/10.1007/s10895-018-2278-4
119. Wang Y, Hao X, Liang L et al (2020) A coumarin-containing Schiff base fluorescent probe with AIE effect for the copper (II) ion. RSC Adv 10:6109–6113. https://doi.org/10.1039/C9RA10632D
120. Kowser Z, Jin C-C, Jiang X et al (2016) Fluorescent turn-on sensors based on pyrene-containing Schiff base derivatives for Cu^{2+} recognition: spectroscopic and DFT computational studies. Tetrahedron 72:4575–4581. https://doi.org/10.1016/j.tet.2016.06.017
121. Slassi S, Aarjane M, El-Ghayoury A, Amine A (2019) A highly turn-on fluorescent CHEF-type chemosensor for selective detection of Cu^{2+} in aqueous media. Spectrochim Acta Part A Mol Biomol Spectrosc 215:348–353. https://doi.org/10.1016/j.saa.2019.02.099
122. Uyanik I, Oguz M, Bhatti AA et al (2017) A new piperidine derivatized-schiff base based "turn-on" Cu^{2+} chemo-sensor. J Fluoresc 27:791–797. https://doi.org/10.1007/s10895-016-2013-y
123. Wu W-N, Mao P-D, Wang Y et al (2018) AEE active Schiff base-bearing pyrene unit and further Cu^{2+}–induced self-assembly process. Sens Actuators B Chem 258:393–401. https://doi.org/10.1016/j.snb.2017.11.114
124. Xu Y, Aderinto SO, Wu H et al (2017) A highly selective fluorescent chemosensor based on naphthalimide and Schiff base units for Cu^{2+} detection in aqueous medium. Z Naturforsch B 72:35–41. https://doi.org/10.1515/znb-2016-0138
125. Zhang Y-M, Zhu W, Qu W-J et al (2018) Novel chemosensor for ultrasensitive dual-channel detection of Cu^{2+} and its application in IMPLICATION logic gate. J Lumin 202:225–231. https://doi.org/10.1016/j.jlumin.2018.05.064
126. Zhang X-B, Han Z-X, Fang Z-H et al (2006) 5,10,15-Tris (pentafluorophenyl)corrole as highly selective neutral carrier for a silver ion-sensitive electrode. Anal Chim Acta 562:210–215. https://doi.org/10.1016/j.aca.2006.01.056
127. He ZL, Yang XE, Stoffella PJ (2005) Trace elements in agroecosystems and impacts on the environment. J Trace Elem Med Biol 19:125–140. https://doi.org/10.1016/j.jtemb.2005.02.010
128. Ratte HT (1999) Bioaccumulation and toxicity of silver compounds: A review. Environ Toxicol Chem 18:89–108. https://doi.org/10.1002/etc.5620180112
129. Chopra I (2007) The increasing use of silver-based products as antimicrobial agents: a useful development or a cause for concern? J Antimicrob Chemother 59:587–590. https://doi.org/10.1093/jac/dkm006
130. Purcell TW, Peters JJ (1998) Sources of silver in the environment. Environ Toxicol Chem 17:539–546. https://doi.org/10.1002/etc.5620170404
131. Bhuvanesh N, Suresh S, Kumar PR et al (2018) Small molecule "turn on" fluorescent probe for silver ion and application to bio-imaging. J Photochem Photobiol A 360:6–12. https://doi.org/10.1016/j.jphotochem.2018.04.027
132. Sahu M, Kumar Manna A, Rout K et al (2020) A highly selective thiosemicarbazone based Schiff base chemosensor for colorimetric detection of Cu2+ and Ag+ ions and turn-on fluorometric detection of Ag^{+} ions. Inorganica Chim Acta 508:119633. https://doi.org/10.1016/j.ica.2020.119633
133. Satarug S, Baker JR, Urbenjapol S et al (2003) A global perspective on cadmium pollution and toxicity in non-occupationally exposed population. Toxicol Lett 137:65–83. https://doi.org/10.1016/S0378-4274(02)00381-8
134. Singh BR, McLaughlin MJ (1999) Cadmium in soils and plants. In: McLaughlin MJ, Singh BR (eds) Cadmium in Soils and Plants. Springer, Netherlands, Dordrecht, pp 257–267

135. Dobson S (1992) Cadmium-environmental aspects. Environ Health Criteria 135:1–156
136. Mohanasundaram D, Bhaskar R, GangatharanVinoth Kumar G et al (2021) A quinoline based Schiff base as a turn-on fluorescence chemosensor for selective and robust detection of Cd^{2+} ion in semi-aqueous medium. Microchem J 164:106030. https://doi.org/10.1016/j.microc.2021.106030
137. Khan SA, Ullah Q, Almalki ASA et al (2021) Synthesis and photophysical investigation of (BTHN) Schiff base as off-on Cd^{2+} fluorescent chemosensor and its live cell imaging. J Mol Liq 328:115407. https://doi.org/10.1016/j.molliq.2021.115407
138. Singh AK, Gupta VK, Gupta B (2007) Chromium(III) selective membrane sensors based on Schiff bases as chelating ionophores. Anal Chim Acta 585:171–178. https://doi.org/10.1016/j.aca.2006.11.074
139. Latva S, Jokiniemi J, Peräniemi S, Ahlgrén M (2003) Separation of picogram quantities of Cr(III) and Cr(VI) species in aqueous solutions and determination by graphite furnace atomic absorption spectrometry. J Anal AtSpectrom 18:84–86. https://doi.org/10.1039/B207941K
140. McRae R, Bagchi P, Sumalekshmy S, Fahrni CJ (2009) In situ imaging of metals in cells and tissues. Chem Rev 109:4780–4827. https://doi.org/10.1021/cr900223a
141. Abbaspour A (2001) Chromium(III) ion-selective electrode based on 4-dimethylaminoazobenzene. Talanta 53:1009–1013. https://doi.org/10.1016/S0039-9140(00)00593-2
142. O'Brien T, Mandel HG, Pritchard DE, Patierno SR (2002) Critical role of chromium (Cr)−DNA interactions in the formation of Cr-induced polymerase arresting lesions. Biochemistry 41:12529–12537. https://doi.org/10.1021/bi020452j
143. Chalmardi GB, Tajbakhsh M, Bekhradnia A, Hosseinzadeh R (2017) A highly sensitive and selective novel fluorescent chemosensor for detection of Cr^{3+} based on a schiff base. Inorganica Chim Acta 462:241–248. https://doi.org/10.1016/j.ica.2017.03.041
144. Chalmardi GB, Tajbakhsh M, Hasani N, Bekhradnia A (2018) A new Schiff-base as fluorescent chemosensor for selective detection of Cr^{3+}: An experimental and theoretical study. Tetrahedron 74:2251–2260. https://doi.org/10.1016/j.tet.2018.03.046
145. Sivaraman G, Sathiyaraja V, Chellappa D (2014) Turn-on fluorogenic and chromogenic detection of Fe(III) and its application in living cell imaging. J Lumin 145:480–485. https://doi.org/10.1016/j.jlumin.2013.08.018
146. Hentze MW, Muckenthaler MU, Galy B, Camaschella C (2010) Two to tango: Regulation of mammalian iron metabolism. Cell 142:24–38. https://doi.org/10.1016/j.cell.2010.06.028
147. Chen M, Xiong H, Wen W et al (2013) Electrochemical biosensors for the assay of DNA damage initiated by ferric ions catalyzed oxidation of dopamine in room temperature ionic liquid. Electrochim Acta 114:265–270. https://doi.org/10.1016/j.electacta.2013.10.122
148. Andersen JET (2005) A novel method for the filterlesspreconcentration of iron. Analyst 130:385. https://doi.org/10.1039/b412061b
149. Halliwell B, Gutteridge JMC (1992) Biologically relevant metal ion-dependent hydroxyl radical generation an update. FEBS Lett 307:108–112. https://doi.org/10.1016/0014-5793(92)80911-Y
150. Yamazaki I, Piette LH (1990) ESR spin-trapping studies on the reaction of Fe^{2+} ions with H_2O_2-reactive species in oxygen toxicity in biology. J Biol Chem 265:13589–13594. https://doi.org/10.1016/S0021-9258(18)77389-4
151. Enami S, Sakamoto Y, Colussi AJ (2014) Fenton chemistry at aqueous interfaces. Proc Natl AcadSci USA 111:623–628. https://doi.org/10.1073/pnas.1314885111
152. Li Y, Pan W, Zheng C, Pu S (2020) A diarylethene derived Fe^{3+} fluorescent chemosensor and its application in wastewater analysis. J Photochem Photobiol A 389:112282. https://doi.org/10.1016/j.jphotochem.2019.112282
153. Faculty of Applied Sciences, UniversitiTeknologi MARA, Hasan S, Zakaria S, Adnan SNAM (2017) Fluorescent chemosensor bearing amine and benzenyl functionality for Fe^{3+} ions detection in aqueous solution. IJCEA 8:28–32. https://doi.org/10.18178/ijcea.2017.8.1.626
154. He Y, Yin J, Wang G (2018) New selective "on-off" fluorescence chemosensor based on carbazole Schiff base for Fe^{3+} detection. Chem Heterocycl Comp 54:146–152. https://doi.org/10.1007/s10593-018-2246-6
155. Khan SA, Asiri AM (2017) Physicochemical properties of novel methyl 2-{(E)-[(2-hydroxynaphthalen-1-yl)methylidene]amino}-4,5,6,7-tetrahydro-1-benzothiophene-3-carboxylate as turn-off fluorometric chemosensor for detection Fe^{3+} ion. J Mol Liq 243:85–90. https://doi.org/10.1016/j.molliq.2017.07.054
156. Harris HH, Pickering IJ, George GN (2003) The chemical form of mercury in fish. Science 301:1203–1203. https://doi.org/10.1126/science.1085941
157. Nolan EM, Lippard SJ (2008) Tools and tactics for the optical detection of mercuric ion. Chem Rev 108:3443–3480. https://doi.org/10.1021/cr068000q
158. Bernhoft RA (2012) Mercury toxicity and treatment: A review of the literature. J Environ Public Health 2012:1–10. https://doi.org/10.1155/2012/460508
159. Carter KP, Young AM, Palmer AE (2014) Fluorescent sensors for measuring metal ions in living systems. Chem Rev 114:4564–4601. https://doi.org/10.1021/cr400546e
160. Tchounwou PB, Ayensu WK, Ninashvili N, Sutton D (2003) Review: Environmental exposure to mercury and its toxicopathologic implications for public health. Environ Toxicol 18:149–175. https://doi.org/10.1002/tox.10116
161. Bhaskar R, Sarveswari S (2020) Thiocarbohydrazide based schiff base as a selective colorimetric and fluorescent chemosensor for Hg^{2+} with "turn-off" fluorescence responses. ChemistrySelect 5:4050–4057. https://doi.org/10.1002/slct.202000652
162. Jiao Y, Zhou L, He H et al (2017) A new fluorescent chemosensor for recognition of Hg^{2+} ions based on a coumarin derivative. Talanta 162:403–407. https://doi.org/10.1016/j.talanta.2016.10.004
163. Jiao Y, Liu X, Zhou L et al (2017) A Schiff-base dual emission ratiometric fluorescent chemosensor for Hg^{2+} ions and its application in cellular imaging. Sens Actuators B Chem 247:950–956. https://doi.org/10.1016/j.snb.2017.01.124
164. Su Q, Niu Q, Sun T, Li T (2016) A simple fluorescence turn-on chemosensor based on Schiff-base for Hg^{2+}-selective detection. Tetrahedron Lett 57:4297–4301. https://doi.org/10.1016/j.tetlet.2016.08.031
165. Wang A, Fan R, Dong Y et al (2017) Novel hydrogen-bonding cross-linking aggregation-induced emission: Water as a fluorescent "ribbon" detected in a wide range. ACS Appl Mater Interfaces 9:15744–15757. https://doi.org/10.1021/acsami.7b01254
166. Wang A, Fan R, Wang P et al (2017) Research on the mechanism of aggregation-induced emission through supramolecular metal-organic frameworks with mechanoluminescent properties and application in press-jet printing. Inorg Chem 56:12881–12892. https://doi.org/10.1021/acs.inorgchem.7b01687
167. Srivastava SK, Gupta VK, Jain S (1995) Determination of lead using a poly(vinyl chloride)-based crown ether membrane. Analyst 120:495. https://doi.org/10.1039/an9952000495
168. Chai F, Wang C, Wang T et al (2010) Colorimetric detection of Pb^{2+} using glutathione functionalized gold nanoparticles. ACS Appl Mater Interfaces 2:1466–1470. https://doi.org/10.1021/am100107k
169. Karachi N, Azadi O, Razavi R et al (2018) Combinatorial experimental and DFT theoretical evaluation of a nano novel thio-dicarboxaldehyde based Schiff base supported on a thin polymer film as a chemosensor for Pb^{2+} detection. J Photochem

Photobiol A 360:152–165. https://doi.org/10.1016/j.jphotochem.2018.04.039
170. Sun T, Niu Q, Guo Z, Li T (2017) A simple highly sensitive and selective turn-on fluorescent chemosensor for the recognition of Pb^{2+}. Tetrahedron Lett 58:252–256. https://doi.org/10.1016/j.tetlet.2016.12.022
171. Hariharan PS, Anthony SP (2014) Selective turn-on fluorescence for Zn^{2+} and $Zn^{2+}Cd^{2+}$ metal ions by single Schiff base chemosensor. Anal Chim Acta 848:74–79. https://doi.org/10.1016/j.aca.2014.07.042
172. Chandra R, Manna AK, Sahu M et al (2020) Simple salicylaldimine-functionalized dipodal bis schiff base chromogenic and fluorogenic chemosensors for selective and sensitive detection of Al^{3+} and Cr^{3+}. Inorganica Chim Acta 499:119192. https://doi.org/10.1016/j.ica.2019.119192
173. Zhu W, Yang L, Fang M et al (2015) New carbazole-based schiff base: Colorimetric chemosensor for Fe^{3+} and fluorescent turn-on chemosensor for Fe^{3+} and Cr^{3+}. J Lumin 158:38–43. https://doi.org/10.1016/j.jlumin.2014.09.020
174. Yin P, Niu Q, Liu J et al (2021) A new AIEE-active carbazole based colorimetric/fluorimetric chemosensor for ultra-rapid and nano-level determination of Hg^{2+} and Al^{3+} in food/environmental samples and living cells. Sens Actuators B Chem 331:129418. https://doi.org/10.1016/j.snb.2020.129418
175. Zhang S, Wu X, Niu Q et al (2017) Highly selective and sensitive colorimetric and fluorescent chemosensor for rapid detection of Ag^{+}, Cu^{2+} and Hg^{2+} based on a simple schiff base. J Fluoresc 27:729–737. https://doi.org/10.1007/s10895-016-2005-y
176. Zhang S, Niu Q, Lan L, Li T (2017) Novel oligothiophene-phenylamine based Schiff base as a fluorescent chemosensor for the dual-channel detection of Hg^{2+} and $Cu^{2+}$with high sensitivity and selectivity. Sens Actuators B Chem 240:793–800. https://doi.org/10.1016/j.snb.2016.09.054
177. Dong G, Duan K, Zhang Q, Liu Z (2019) A new colorimetric and fluorescent chemosensor based on schiff base-phenyl-crown ether for selective detection of Al^{3+} and Fe^{3+}. Inorganica Chim Acta 487:322–330. https://doi.org/10.1016/j.ica.2018.12.036
178. Dong Y, Fan R, Chen W et al (2017) A simple quinolone Schiff-base containing CHEF based fluorescence 'turn-on' chemosensor for distinguishing Zn^{2+} and Hg^{2+} with high sensitivity, selectivity and reversibility. Dalton Trans 46:6769–6775. https://doi.org/10.1039/C7DT00956A
179. Gao W, Zhang Y, Li H, Pu S (2018) A multi-controllable selective fluorescent turn-on chemosensor for Al^{3+} and Zn^{2+} based on a new diarylethene with a 3-(4-methylphenyl)-1H-pyrazol-5-amine Schiff base group. Tetrahedron 74:6299–6309. https://doi.org/10.1016/j.tet.2018.09.017
180. Horak E, Vianello R, Hranjec M, Murković Steinberg I (2018) Colourimetric and fluorimetric metal ion chemosensor based on a benzimidazole functionalised Schiff base. Supramol Chem 30:891–900. https://doi.org/10.1080/10610278.2018.1436708
181. İnal EK (2020) A fluorescent chemosensor based on schiff base for the determination of Zn^{2+}, $Cd^{2+}$and Hg^{2+}. J Fluoresc 30:891–900. https://doi.org/10.1007/s10895-020-02563-6
182. Iyappan M, Dhineshkumar E, Anbuselvan C (2020) Novel schiff base of E-2-(((4-aminophenyl)imino)methyl)-5-(difluoromethoxy)phenol fluorescence chemosensor for detection of Al^{3+}, Fe^{2+}, Cu^{2+} ions and its application towards live cell imaging. Asian J Chem 32:739–745. https://doi.org/10.14233/ajchem.2020.22394
183. Purkait R, Dey S, Sinha C (2018) A multi-analyte responsive chemosensor vanilinyl Schiff base: fluorogenic sensing of Zn(II), Cd(II) and I^{-}. New J Chem 42:16653–16665. https://doi.org/10.1039/C8NJ03165G
184. Roy N, Dutta A, Mondal P et al (2017) Coumarin based fluorescent probe for colorimetric detection of Fe^{3+} and fluorescence turn on-off response of Zn^{2+} and Cu^{2+}. J Fluoresc 27:1307–1321. https://doi.org/10.1007/s10895-017-2065-7
185. Tajbakhsh M, Chalmardi GB, Bekhradnia A et al (2018) A new fluorene-based schiff-base as fluorescent chemosensor for selective detection of Cr^{3+} and Al^{3+}. Spectrochim Acta Part A Mol Biomol Spectrosc 189:22–31. https://doi.org/10.1016/j.saa.2017.08.007
186. Mandal J, Ghorai P, Pal K et al (2019) 2-hydroxy-5-methylisophthalaldehyde based fluorescent-colorimetric chemosensor for dual detection of Zn^{2+} and Cu^{2+} with high sensitivity and application in live cell imaging. J Lumin 205:14–22. https://doi.org/10.1016/j.jlumin.2018.08.080
187. Wang L, Li W, Zhi W et al (2018) A new coumarin Schiff based fluorescent-colorimetric chemosensor for dual monitoring of Zn^{2+} and Fe^{3+} in different solutions: An application to bioimaging. Sens Actuators B Chem 260:243–254. https://doi.org/10.1016/j.snb.2017.12.200
188. Kaur N, Kaur B (2020) Colorimetric and fluorescent multi-ion recognition by Anthracene appended di-Schiff base chemosensor. Inorg Chem Commun 121:108239. https://doi.org/10.1016/j.inoche.2020.108239
189. Iyappan M, Dhineshkumar E, Anbuselvan C (2020) Schiff base of 4E,10E–4-(2-(4-nitrophenyl)-N-((1H-indol-3-yl) methylene) benzenamine-based "turn-on" fluorescence chemosensor for highly selective detection of Ni^{2+}, Fe^{3+} and Mg^{2+} ions. Chem Pap 74:4213–4226. https://doi.org/10.1007/s11696-020-01236-9
190. Manna AK, Rout K, Chowdhury S, Patra GK (2019) A dual-mode highly selective and sensitive schiff base chemosensor for fluorescent colorimetric detection of Ni^{2+} and colorimetric detection of Cu^{2+}. Photochem Photobiol Sci 18:1512–1525. https://doi.org/10.1039/C9PP00114J
191. Rout K, Manna AK, Sahu M et al (2019) Triazole-based novel bis Schiff base colorimetric and fluorescent turn-on dual chemosensor for Cu^{2+} and Pb^{2+}: application to living cell imaging and molecular logic gates. RSC Adv 9:25919–25931. https://doi.org/10.1039/C9RA03341F
192. Kaczmarek MT, Zabiszak M, Nowak M, Jastrzab R (2018) Lanthanides: Schiff base complexes, applications in cancer diagnosis, therapy, and antibacterial activity. Coord Chem Rev 370:42–54. https://doi.org/10.1016/j.ccr.2018.05.012
193. Kundu BK, Mandal P, Mukhopadhyay BG et al (2019) Substituent dependent sensing behavior of Schiff base chemosensors in detecting $Zn^{2+}$and Al^{3+} ions: Drug sample analysis and living cell imaging. Sens Actuators B Chem 282:347–358. https://doi.org/10.1016/j.snb.2018.11.076
194. Singh B, Moudgil L, Singh G, Kaura A (2018) The growth of ZnO nanostructures using Arginine. Bikaner, India, p 030234
195. Mahal A, Goshisht MK, Khullar P et al (2014) Protein mixtures of environmentally friendly zein to understand protein–protein interactions through biomaterials synthesis, hemolysis, and their antimicrobial activities. Phys Chem Chem Phys 16:14257–14270. https://doi.org/10.1039/C4CP01457J
196. Cui M, Xin Y, Song R et al (2020) Fluorescence sensor for bovine serum albumin detection based on the aggregation and release of CdS QDs within CMC. Cellulose 27:1621–1633. https://doi.org/10.1007/s10570-019-02865-4
197. Zhu B, Zhang X, Jia H et al (2010) A highly selective ratiometric fluorescent probe for 1,4-dithiothreitol (DTT) detection. Org Biomol Chem 8:1650. https://doi.org/10.1039/b923754b
198. Gupta KC, Sutar AK (2008) Catalytic activities of Schiff base transition metal complexes. Coord Chem Rev 252:1420–1450. https://doi.org/10.1016/j.ccr.2007.09.005

199. Ma C, Xu B, Xie G et al (2014) An AIE-active luminophore with tunable and remarkable fluorescence switching based on the piezo and protonation–deprotonation control. Chem Commun 50:7374–7377. https://doi.org/10.1039/C4CC01012D
200. Yoon B, Lee J, Park IS et al (2013) Recent functional material based approaches to prevent and detect counterfeiting. J Mater Chem C 1:2388. https://doi.org/10.1039/c3tc00818e
201. Ling P-X, Fang S-L, Yin X-S et al (2015) Palladium-catalyzed arylation of unactivated γ-Methylene C(sp3)-H and δ-C-H bonds with an oxazoline-carboxylate auxiliary. Chem Eur J 21:17503–17507. https://doi.org/10.1002/chem.201502621